ISSN 0024-4902, Lithology and Mineral Resources, 2021, Vol. 56, No. 6, pp. 487–508. © Pleiades Publishing, Inc., 2021.
Russian Text © The Author(s), 2021, published in Litologiya i Poleznye Iskopaemye, 2021, No. 6, pp. 513–537.

Carbonate Sedimentology of the Upper Riphean (Neoproterozoic) Uk Formation, Southern Urals

S. A. Dub[a, *] and D. V. Grazhdankin[b, c, **]

[a] *Zavaritsky Institute of Geology and Geochemistry, Ural Branch, Russian Academy of Sciences, Yekaterinburg, 620016 Russia*
[b] *Trofimuk Institute of Petroleum Geology and Geophysics, Siberian Branch, Russian Academy of Sciences, Novosibirsk, 630090 Russia*
[c] *Novosibirsk State University, Novosibirsk, 630090 Russia*
**e-mail: sapurins@gmail.com*
***e-mail: dima.grazhdankin@gmail.com*

Received November 17, 2020; revised January 15, 2021; accepted June 29, 2021

Abstract—Lithological characteristics and results of the lithofacies analysis of carbonate deposits in the most complete section of the Upper Uk Subformation of the Riphean stratotype (northern part of the Bashkir Anticlinorium, southern Urals) are presented. The subformation is divided into the following members or sequences (from the bottom to top): Yuryuzan, Medved I, Manaysu, and Medved II. The subformation bottom occurs at the base of a huge stromatolite buildup. The Yuryuzan member is characterized by the thin-columnar branching stromatolites *Patomella*. The Medved I and Medved II members are represented mainly by bioherms consisting of the columnar-branching stromatolites *Linella*, interbiohermal rocks, and local packets of layered granular limestones found only in the lower member). The Manaysu member comprises layered (mainly cyclic) deposits with abundant molar tooth (MT) structures. The growth of the Yuryuzan member stromatolites occurred most likely in the upper subtidal-peritidal zone within the inner carbonate ramp under the influence of siliciclastic-bearing currents. Stromatolite buildups in Medved I and Medved II members were formed as a part of wide facies belts below the normal wave base (inner/middle ramp boundary) but within the photic zone. Layered limestones in the Medved I member are periodic storm current deposits. Environments of the inner ramp and upper middle ramp dominated during the deposition of Manaysu sediments with signatures of the influence of normal and storm waves. The sequence including the upper part of the Lower Uk Subformation, as well as the Yuryuzan and Medved I members of the Upper Uk Subformation, reflects a progressive deepening of the basin. The later slowdown in the rate of sea level rise (or fall) fostered the change in facies and the formation of the shallow-water Manaysu member. Subsequently, the transgressive trend appeared again, resulting in the formation of Medved II member. The upper boundary of the Uk Formation corresponds to a major break in the geological record associated with global glaciation.

Keywords: Bashkir Anticlinorium, Upper Riphean, carbonate ramp, stromatolites, MT structures, tempestites, facies

DOI: 10.1134/S0024490221060031

INTRODUCTION

Late Precambrian carbonate platforms are characterized by specific features discriminating them from similar but noncoeval geological bodies. In particular, it is believed that the Neoproterozoic is characterized by carbonate ramps, diverse organogenic buildups, specific assemblages of branching stromatolites, rocks with giant ooids, and abundant calcimicrobes (Grotzinger and James, 2000 and references therein).

Upper Precambrian carbonate sections exposed on the western slope of the southern Urals within the Bashkir Anticlinorium (BA) include rocks with well-preserved sedimentogenic structures, providing a detailed insight into the ancient depositional environment. Such objects undoubtedly need a comprehensive state-of-the-art study. The Upper Riphean (Neoproterozoic in the International Stratigraphic Chart) Uk Formation is among such objects.

The Uk Formation crowning the Karatau Group section in the Riphean stratotype (Bekker, 1961; Maslov et al., 2001; Puchkov et al., 2017) lies above the Min'yar Formation with a hiatus (Kuznetsov et al., 2006, 2014; Maslov, 2020). It is divided into two subformations: lower terrigenous-carbonate Kul'tamak and upper carbonate-rich Aktash (Bekker, 1961; Kozlov, 1982; Maslov et al., 2001, 2019; *Stratotip* ..., 1983). The Uk Formation is as much as 450 m thick in the most complete sections, according to (Kozlov, 1982).

The Uk Formation includes stromatolites *Linella ukka* Krylov, *Linella simica* Krylov, *Tungussia bassa* Krylov, and *Patomella kelleri* Raaben (Krylov, 1967; *Stratotip* ..., 1982). According to T. Jankauskas and A. Veis, microbiota in the Uk Formation is characterized by the abundant *Leiosphaeridia*, *Protosphaeridium*, and *Siphonophycus typicum* along with *Palaeolyngbya zilimica*, *Bavlinella faveolata,* and *Symplassosphaeridium* sp., as well as sheaths of *Polytrichoides* and *Tortunema* (Sergeev, 2006; Stanevich et al., 2018; *Stratotip* ..., 1982; Veis et al., 2003). According to (Sergeev et al. 2010), this microfossil assemblage is marked by low taxonomic diversity (relative to the Min'yar Formation) and wide stratigraphic distribution range.

Based on the glauconite dating by the Rb–Sr and K–Ar methods, the Lower Uk Subformation is estimated at 663 ± 9 and 669 ± 16 Ma (Zaitseva et al., 2008). The geological data, however, suggest that the Uk Formation is older than ~717 Ma (Maslov et al., 2019). In particular, the Uk Formation shows structural features much more similar to the underlying rocks than the unconformably overlying sequences, and the overlying Bakeevo Formation is estimated at 642 ± 9 Ma (Zaitseva et al., 2019). In some geological structures of BA (e.g., Tolparovo trough and Krivaya Luka syncline), Uk Formation deposits are eroded (Gorozhanin et al., 2019; *Gosudarstvennaya* ..., 2013). On the eastern limb of BA, the Karatau Group is overlain by the Arsha Group (Kozlov et al., 2011; Puchkov et al., 2017), with the lower level of tillites formed probably during the Sturtian Glaciation. In limestones of the Upper Uk Subformation, the range of $^{87}Sr/^{86}Sr$ values satisfying the geochemical criteria for isotope system preservation is 0.70535–0.70611 (Kuznetsov et al., 2006). Such isotope values are typical for the pre-Cryogenian deposits, as suggested in (Zaky et al., 2019). In addition, the Upper Uk Subformation is characterized by a sequence with abundant molar tooth (MT) structures that almost completely disappear from the geological record after the Sturtian Glaciation onset (Hodgskiss et al., 2018; Shields, 2002; and others). Correspondingly, the Uk Formation belongs more likely to the Tonian System in the International Stratigraphic Chart.

OBJECT AND METHODS

One of the most complete and accessible sections of the Uk Formation is represented by the Medved section exposed on the slope of Mt. Medved in the eastern outskirts of Ust-Katav (Shubino Settlement, Chelyabinsk region) and assigned in terms of tectonics to the western limb of the Suleimanov anticline in BA (Fig. 1). Description of this section and the results of previous studies are presented in (Bekker, 1961; Domrachev, 1952; Kozlov, 1982; Krylov, 1967, 1975; Kuznetsov et al., 2006; Maslov et al., 2001b; *Putevoditel* ..., 1995; *Stratotip* ..., 1982, 1983; and others). In recent years, we scrutinized the lithology and geochemistry of the Upper Uk Subformation in this section. Main features of the dominating lithotypes and carbonate facies were deciphered. Distribution of rare elements revealed that the depositional environment was depleted in oxygen. Information suggesting the existence of prokaryotic and eukaryotic communities in the paleobasin was obtained (Dub and Grazhdankin, 2018; Dub et al., 2019; Maslov et al., 2019; Parfenova and Mel'nik, 2020).

The present communication addresses the following issues: textures and structures of the Upper Uk Subformation rocks; spatial distribution of different microfacies; lithotypes and facies of limestones; architecture of the carbonate platform; and reconstruction of the depositional environment and their evolution. The lack of fractures and good exposure of the study area made it possible to study the Uk Formation along different cross-sections. It was revealed previously that the Upper Uk Subformation is characterized by facies heterogeneity. Therefore, its description along profiles spaced apart for more than 10 m can differ significantly (Dub and Grazhdankin, 2018). To compile a comprehensive description of this section, we defined the most contrast sequences during field works, making it possible to scrutinize their lithology and trace them along the lateral direction.

We took samples from all exposed lithotypes and scrutinized transitions between them. We followed the following concept of V. Frolov (1984): "lithotype" is a typical rock (layer or group of similar layers) with a stable assemblage of signatures testifying to its formation mechanism and conditions; "genetic type" includes rocks formed by a specific mechanism (or produced by a specified geological process); the term "facies" is applied to rocks with signatures of the depositional environment but not to the environment itself.

Laboratory studies after field works were devoted mainly to the microfacies analysis (Flügel, 2010). Identification of limestone texture was based the classification proposed by (Dunham, 1962) modified in (Embry and Klovan, 1971; Lokier and Junaibi, 2016; Wright, 1992). Since major features of the microfacies are deciphered mainly during the petrographic examination of thin sections, microfacies represents the smallest component of facies, and a specified layer in the section can comprise one or several microfacies. In practice, researchers usually deal with microfacies types that are distinguished only based on the most typical properties (Flügel, 2010) and, thus, are similar to lithotypes in broad sense. Combination of the Russian and foreign methods made it possible to integrate the cogenetic and similar microfacies into microfacies types that commonly correspond to lithotypes.

The majority of lithotypes were identified during field works. The facies were identified based on the analysis of paragenetic associations of lithotypes. Examination of facies assemblages, in turn, provided

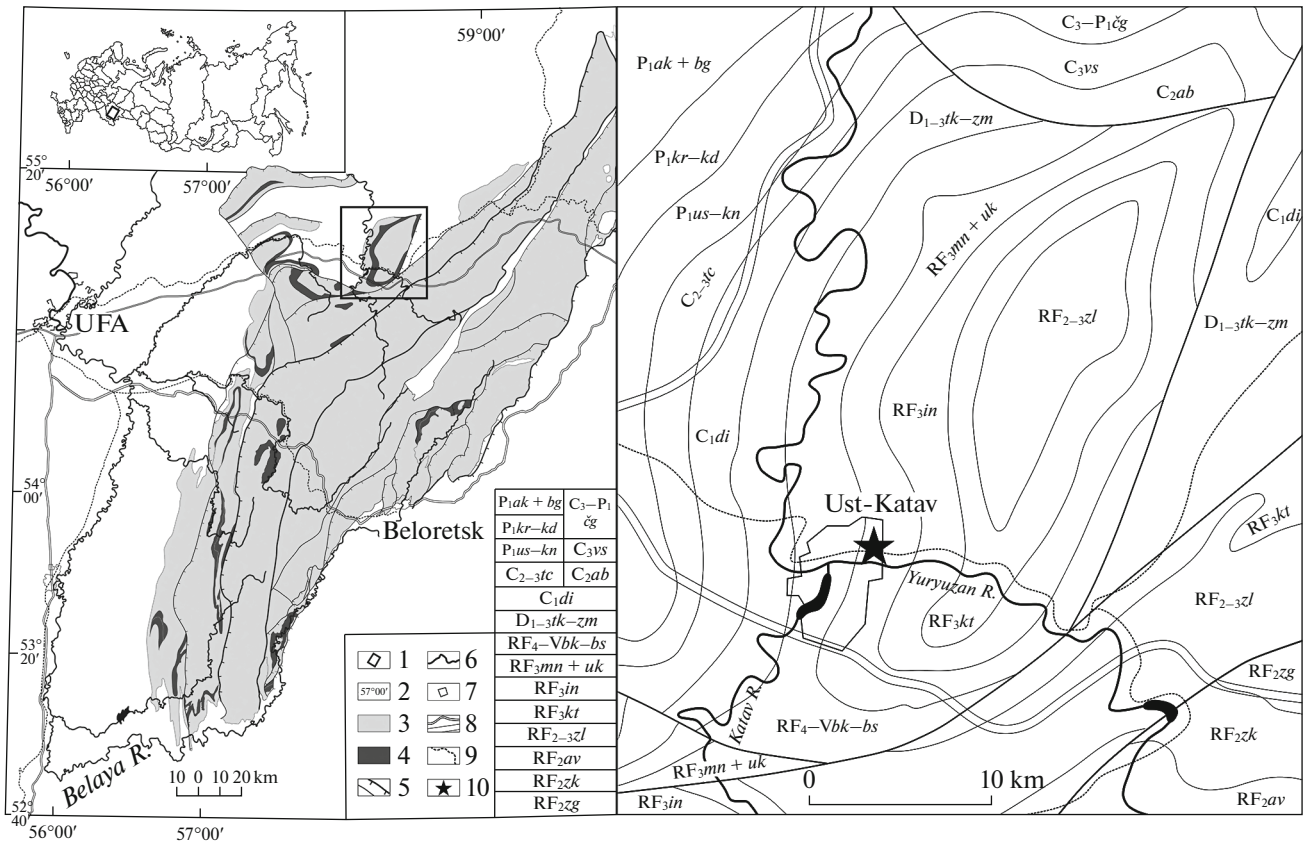

Fig. 1. Boundaries of the Bashkir Anticlinorium along the top of Precambrian rocks (left) and location of the studied section in the detailed geological map (right). (1) Sector provided with the detailed geological map, (2) coordinates, (3) area of Precambrian rocks (except the Min'yar and Uk formations) in BMA, (4) area of undifferentiated Min'yar and Uk formations, (5) tectonic boundaries, (6) rivers, (7) populated sites, (8) highways, (9) railways, (10) profile "Medved". Stratigraphic subdivisions: (RF_2) Middle Riphean—(zg) Zigal'ga Formation, (zk) Zigaza–Komarovo Formation, (av) Avzyan Formation (Group); (RF_{2-3}) Middle–Upper Riphean—(zl) Zil'merdak Formation (Group); (RF_3) Upper Riphean—(kt) Katav Formation, (in) Inzer Formation, (mn+uk) Min'yar and Uk formations; (RF_4—Vbk–bs) Terminal Riphean–Vendian Bakeevo–Basa formation interval; (D_1–$_3$ tk–zm) Devonian Takata Formation–Zilim Group interval; (C) Carboniferous, (di) dolomite–limestone section, (tc) terrigenous–carbonate section, (ab) Abdrezyakovo Formation, (vs) Veselga strata; (C_3–P_1čg) Upper Carboniferous–Lower Permian Chigishan Formation; (P_1) Lower Permian, (us–kn) Uskalyk and Kurmain formations, (kr–kd) Karamura–Kondurovo formation interval, (ak+bg) Aktasta and Baigendzha formations, modified after (*Gosudarstvennaya* ..., 2013).

insight into the functioning of sedimentary system of the Uk Formation, and its temporal transformation was traced based on the change of sequences along the section.

DESCRIPTION OF THE UPPER UK SUBFORMATION SECTION

Overview of Sequences

The Upper Uk Subformation (about 150 m thick) is represented in the Medved section mainly by gray, light gray, and dark gray stromatolitic bioherm limestones with lenses of the thin-layered micrograined varieties, as well as layered packets of coarse-grained limestones. Rocks are dolomitized to a variable extent. Terrigenous–carbonate rocks are only typical for the subformation bottom, whereas carbonate–argillaceous varieties (usually green or dark gray, up to black in some places) occur as subordinate components at higher stratigraphic levels. The subformation is divided into four members (from the bottom to top): Yuryuzan, Medved I, Manaysu, and Medved II (Fig. 2a).

The upper part of the underlying Lower Uk Subformation is represented by gray layered siltstones and fine-grained sandstones with numerous interlayers of micrograined, intraclastic, or containing abundant MT structures limestones. Glauconite often confined to the bedding surfaces.

Yuryuzan member (exposure on the right bank of the Yuryuzan River above the Ust-Katav Settlement) is transitional from the terrigenous–carbonate Lower Uk Subformation to the carbonate-rich Upper Uk Subformation. The lower boundary of the member is established at the base of the massive limestones composed mainly of columnar stromatolites *Patomella* and lying above distinctly layered rocks of the Lower Uk

Subformation (Fig. 2b). The rocks are intensely dolomitized. The member is exposed fragmentarily, but all outcrops are represented by the stromatolitic limestones, probably, due to the existence of a single large organogenic buildup. Thickness of the member is as much as 25 m.

The thickest and well-exposed sequence in the studied section is represented by **Medved I member** named thus because of its location on the slope of Mt. Medved. The sequence is composed of massive stromatolitic buildups separated from each other by the layered rock packets or rare argillaceous–carbonate rock interlayers traced along the lateral direction over tens of meters or more. The organogenic buildups comprise conjugated bioherms composed of columnar stromatolites *Linella* (previously identified "species" *Linella ukka*, *Linella simica*, and *Tungussia bassa* should be considered as varieties of *Linella*). The interbiohermal space in buildups is filled with micrograined limestone lenses sometimes with the clay material admixture. The size (diameter and height) of bioherms varies from tens of centimeters to a few meters. In some places, they are separated by the carbonate–argillaceous rock strata or lenses, but more often by surfaces emphasizing the rounded shape of these bodies. Substrate for the bioherm growth was represented by other bioherms or coarse-grained limestone beds. The member base is drawn where the dominant form of stromatolites changes (Fig. 2c). Carbonate breccias were not found in the Medved member. This sequence represents a giant biostrome including local layered rock packets. Hierarchical relationships of bodies therein can be presented in the following scheme: (I) stromatolite columns, (II) stromatolite bioherms (set of columns formed during the growth and separation of one microbial colony), (III) organogenic stromatolite buildups (bioherm assemblages), and (IV) huge organogenic stromatolite buildup (together with the Yuryuzan stromatolite buildup). The rocks are marked by a weak and irregular dolomitization, and the micrograined interbiohermal rocks are least dolomitized. Thickness of the member is ~70–75 m.

Manaysu member. The most representative section of the Upper Uk Subformation rocks, similar to rocks of this member, is located 95 km southwest of Ust-Katav near the Kulmasovo Settlement on the Basu River 750 m below the Manaysu Creek mouth. The member lies on an irregular surface (top) of the underlying sequence and is characterized by a layered structure (Fig. 2d). Based on lithology, it is similar to carbonate rocks in the upper part of the Lower Uk Subformation. The Manaysu member is represented by intercalation of distinctly-grained (coarse-grained) and micrograined limestones, but some varieties are dolomitized or weakly silicified. The member is characterized by numerous MT structures, and stromatolites are virtually missing. The upper part (about 11 m) of the member is recrystallized. Thickness of the Manaysu member varies from 22 to 28 m, decreasing on ledges of the underlying organogenic buildups.

Medved II member is similar to Medved I. It is also marked by the presence of stromatolite bioherms but a scarcity of the layered coarse-grained limestones that do not make up prominent packets. The sequence lies above a relatively even top of the Manaysu member. Rocks in the Medved member are considerably recrystallized and dolomitized (Fig. 2e). Thickness is about 15 m.

The studied section is considered a proxy of the Uk Formation (Maslov et al., 2019; *Putevoditel* ..., 1995; and others). Therefore, the proposed scheme of its subdivision can be applied for a detailed correlation of sections located in different tectonic areas (structural-facies zones) of BA.

Yuryuzan Member

The framework of organogenic buildups in this member (Fig. 3a) is composed of branching stromatolites *Patomella*. Thin (up to 1–2 cm across), sinuous columns are arranged freely without any joints. The columns include both subvertical and inclined (up to 50°–60°) individuals (Figs. 3b, 3c). Their cross-section is marked by intricate morphology (Figs. 3d, 3e). In some places, stromatolite columns are slightly thicker, and they resemble stromatolites *Linella* in sectors located immediately below the embranchment level.

Stromatolites are characterized by the intercalation of thin (<1 mm) dark gray cryptograined strata and lighter, fine- to microcrystalline carbonates with an admixture of the terrigenous material (Fig. 3f). The intercolumnar space is filled with the carbonate mass

Fig. 2. Structure of the Medved section (Upper Uk Subformation). (a) Lithological column showing the proportion of different lithotypes (stromatolites, cyclites, and structural components are out of scale): (1) siltstones (argillaceous and carbonate included), (2) micrograined limestones, (3) granular (fine-grained to coarse-grained) limestones with rare larger clasts, (4) stromatolitic limestones with *Linella*, (5) stromatolitic dolomitic limestones with *Patomella*, (6) MT structures of different types; (b) type of contact between the Lower Uk and Upper Uk subformations (distinctly layered deposits are replaced by the massive variety (this member interval is exposed insufficiently); (c) Yuryuzan/Medved I member boundary based on change in the stromatolite complex; (d) inferred Medved I/Manaysu member boundary (a lenticular (?) stromatolite *Linella* bed (2 m thick) detected 4 m above the level marked by the bend of the dashed line); (e) poorly exposed contact between the distinctly layered sediments (Manaysu member) and massive stromatolites (Medved II member). Conditional boundaries of members are shown by white dashed lines. Designations: (R_3) Upper Riphean, (uk_1) Lower Uk Subformation, (uk_2) Upper Uk Subformation, (yur) Yuryuzan member, (md) Medved member: (I) lower, (II) upper; (mns) Manaysu member; (MT) molar tooth structures. Hammer length is 40 cm.

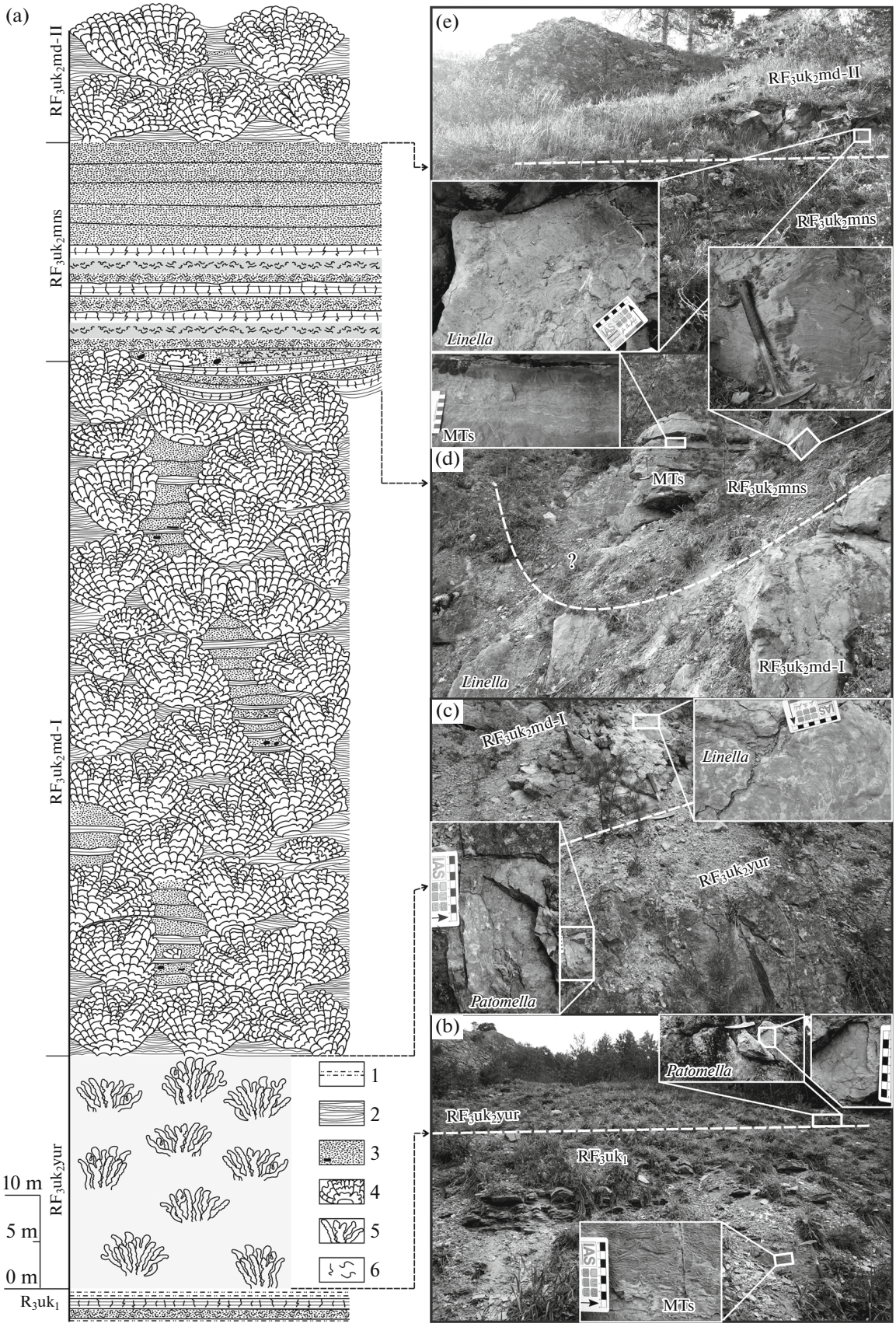
(a)
RF3uk2md-II
RF3uk2mns
RF3uk2md-I
RF3uk2yur
R3uk1
10 m
5 m
0 m
1
2
3
4
5
6
(e)
RF3uk2md-II
RF3uk2mns
Linella
MTs
(d)
MTs
RF3uk2mns
?
Linella
RF3uk2md-I
(c)
RF3uk2md-I
Linella
RF3uk2yur
Patomella
(b)
Patomella
RF3uk2yur
RF3uk1
MTs

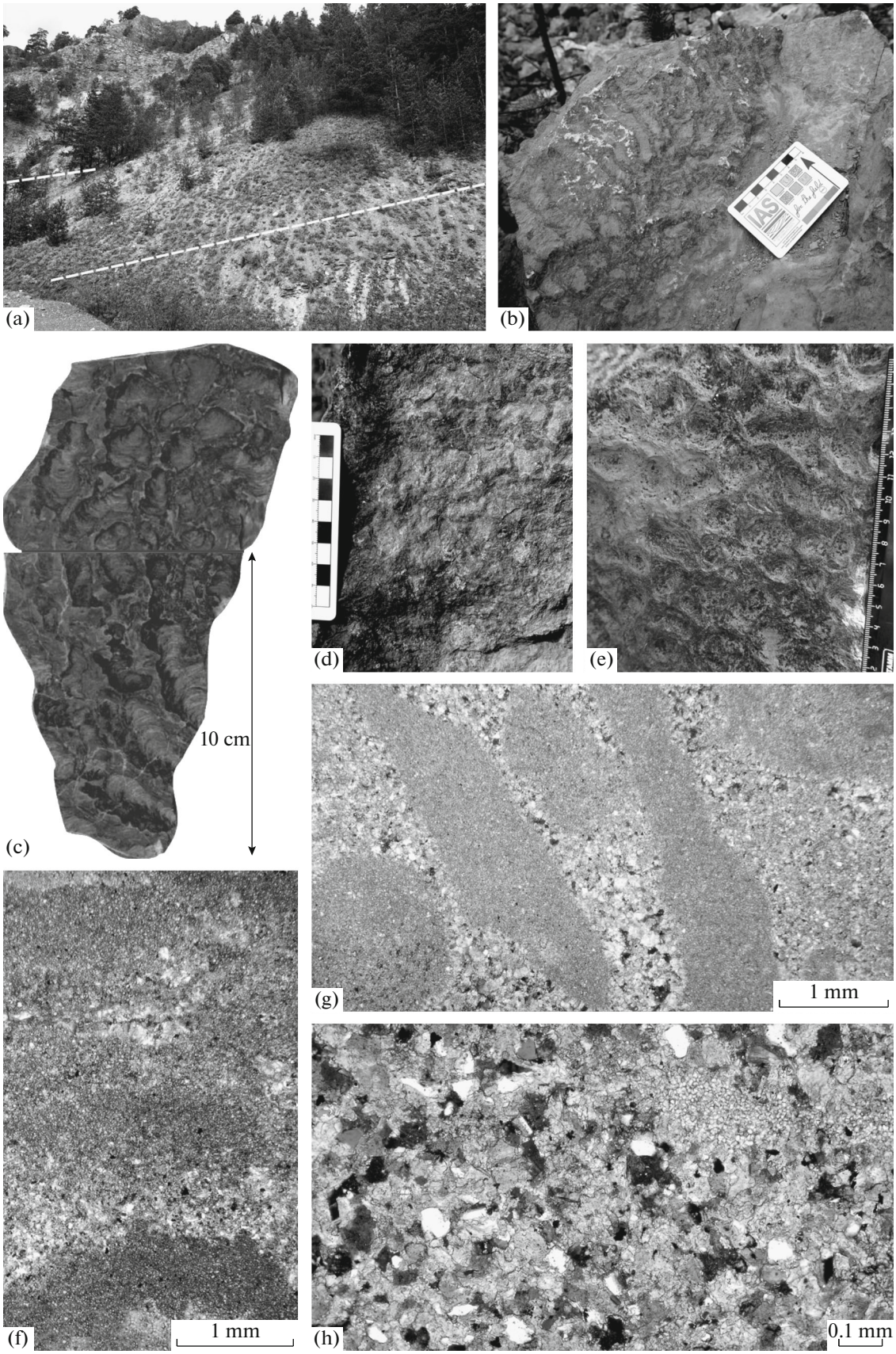
(a)
(b)
(c)
10 cm
(d)
(e)
(f)
1 mm
(g)
1 mm
(h)
0.1 mm

(micrite and sparite) and clastic terrigenous–carbonate material. The rock is dominated by the sand- and gravel-sized carbonate clasts–contiguous intraclasts (Fig. 3g). The noncarbonate mass is represented by the sandy–silty grains of quartz and feldspars, mica flakes, glauconite, and clay minerals (Fig. 3h). Thus, columns *Patomella* are composed of the thin-layered bindstones, while the intercolumn space is filled with the rudstone and packstone intraclasts.

Compact crypto- and microcrystalline dolomite masses are widespread, and the euhedral orthorhombic crystal dissemination is virtually absent. Probably, dolomite occurs mainly in the stromatolite columns and to a lesser extent in host rocks.

Medved I Member

It is composed mainly of stromatolite buildups (Figs. 4, 5). Layered cyclic packets of granular limestones (up to 12 m thick) that extend along the lateral sublatitudinal direction over a small distance (up to 10 m) are found locally (Fig. 4a).

Bioherms in this member are composed of differently oriented columnar stromatolites *Linella*, with the central and peripheral parts dominated, respectively, by the subvertical and subhorizontal individuals (Fig. 4b). In some places, the bioherms are asymmetrical because of the development of unidirectional subhorizontal columns. Distance between the columns in bioherms varies, but usually does not exceed the diameter of columns that are commonly located very close to each other (Figs. 4b, 4c), serving as a fundamental difference between *Linella* and *Patomella*.

Columnar stromatolites are composed of the laminae of dark gray cryptocrystalline (pelitomorphic), as well as light gray and gray microcrystalline, calcite. In thin sections, one can see gradual transitions from the light gray strata to darker varieties in some places. Microcrystalline sectors occupy the largest volume in columns, while the pelitomorphic calcite makes up distinct laminae and lenses (in thin-layered bindstones) or makes up compact clusters associated with fenestra (in nonlayered boundstones). Both varieties can occur in the same column (Fig. 5a).

Clusters are relatively large (commonly <0.5 mm) and most typical for the tilted thin stromatolite columns. In the thicker subvertical individuals, they occur mainly as low-angle irregular tubercles beneath the upper boundaries of dark gray cryptocrystalline masses. Clusters are prominent among the light gray microcrystalline carbonate in the overlying strata (Fig. 5a). Such problematic structures can be defined as calcimicrobes (Fig. 5b).

Organogenic buildups include the microgranular limestone "bodies" delimited by the surrounding bioherm surfaces (Figs. 4d, 4e). They usually comprise the homogeneous calcimudstones with rare thin (up to 0.5 mm) wackestone layers (Fig. 5c). These rocks often contain a variable amount of the fine-dispersed terrigenous admixture. The bedding-parallel fenestra are observed in some places.

Interbiohermal deposits—previously interpreted erroneously as stratified stromatolites or biolaminites (Dub and Grazhdankin, 2018; Maslov et al., 2019)—are characterized mainly by the horizontal-layered and gentle cross-wavy structures (Fig. 4e).

Layered granular limestone packets, which delimit the stromatolites (Figs. 4f–4h), include rocks with different grain sizes ranging from microgranular limestones to calcirudites, are characterized by indistinct graded bedding, and contain occasional flat, differently oriented carbonate clasts of the gravel, pebble, or larger size (Fig. 4g). If packstones (Fig. 5d) and rudstones (Fig. 5e) prevail, these packets also include grainstones, wackestones, and calcimudstones. Very diverse is the set of morphological elements represented mainly by intraclasts. They are composed of the predominant aggregate grains (grapestones?) produced by the multiple reworking of carbonate material; fragments of MT cracks (MT clasts) are widespread; and stromatoclasts and peloids are found in some places (Figs. 5d, 5e). The smallest clasts in the aggregate grains are represented mostly by peloids or peloidal packstones. The MT clasts are deciphered easily in most cases based on the typical light homogeneous holocrystalline microsparite. In some places, they are rounded and included in aggregate grains (Fig. 5e). Some intraclasts and their clusters are often surrounded by the isopachous cement rims of calcite (Fig. 5e). Identification of stromatoclasts is based on the inclusions of specific clusters and the lack of signs of reworking. Homogeneous grains composed of the dark micro- and cryptograined calcite are assigned to peloids.

Components of granular limestones are poorly sorted. The elongated morphological elements are usually differently oriented with a predominance of subhorizontal orientation on some sectors. The fine-grained (more often, peloidal) limestones contain MT cracks at some levels (Fig. 5f).

Fig. 3. Lithological characteristics of Yuryuzan member rocks. (a) General view of the section ((b) longitudinal section of the stromatolite bioherm displaying different spatial orientation of columns; (c) sample 1701-32 with thin-columnar stromatolites *Patomella* with polished surface inclined to the crosscut (bottom) and bedding (top); (d) transverse section of stromatolites *Patomella* (subaerial exposure of the fresh surface over three years); (e) transverse section of stromatolites *Patomella* on the weathered surface; (f–h) photomicrographs of thin sections (sample 1701-32, crossed nicols): (f) longitudinal section of the axial part of a stromatolite column, (g) carbonate intraclasts and terrigenous–carbonate groundmass in the intercolumn space of bioherm, (h) terrigenous sandy–silty grains floating in the intercolumn space of stromatolites.

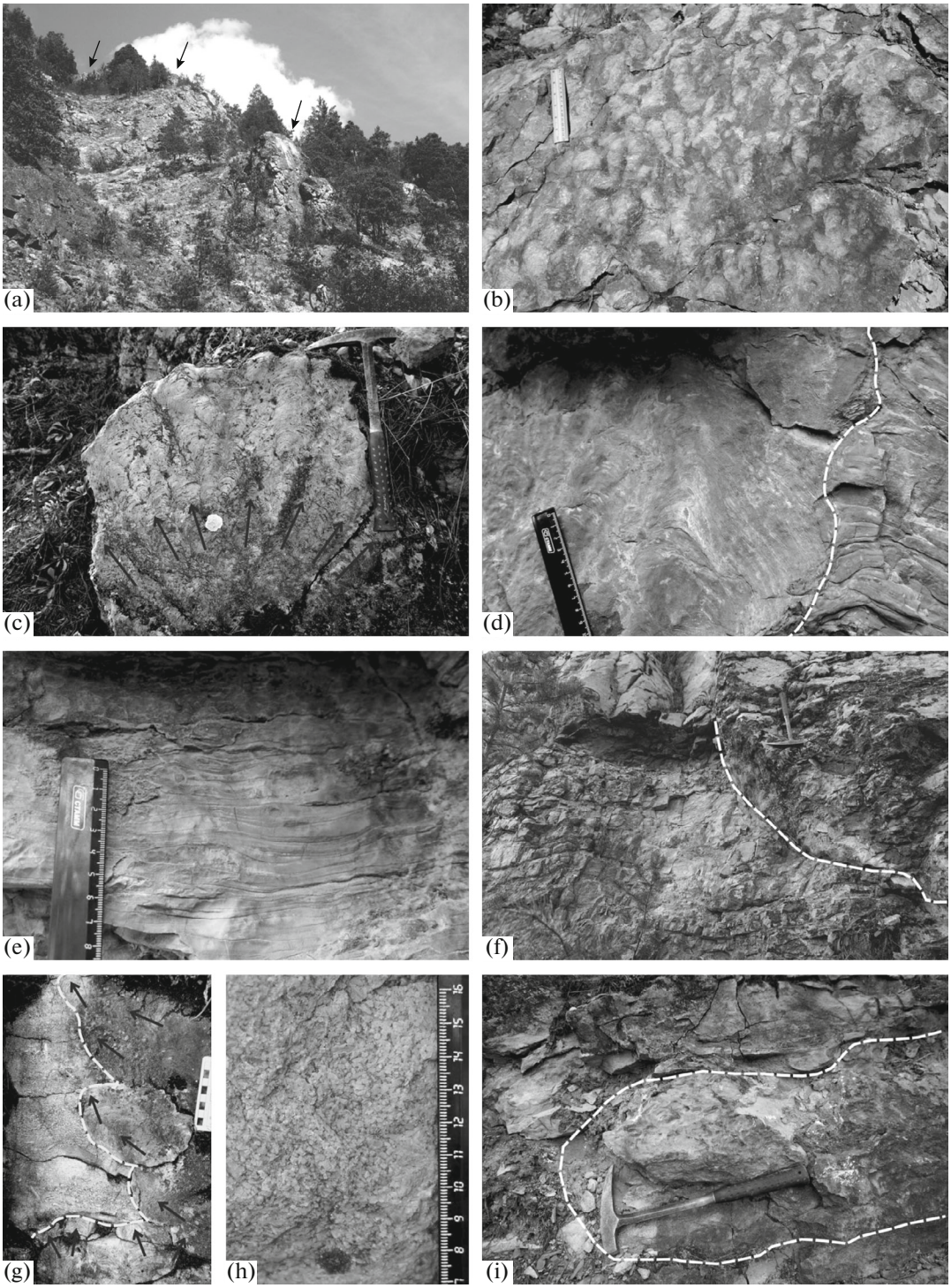

Fig. 4. Lithological characteristics of Medved I member rocks. (a) General view of the section (arrows show the granular limestone packets exposed as jutting rocks in the relief; (b) transverse section of a large bioherm *Linella* in the lower part of the section (dolomitized sectors are confined to the intercolumn contact zones); (c) transverse section of a typical bioherm *Linella* with flabellate axes of the branching columns shown by arrows (columns are often tightly spaced); (d) style of contact (dashed line) of the stromatolitic bioherm with the interbioherm deposits; (e) typical structures of the interbiohermal microgranular deposits; (f) fragment of a layered limestone packet and style of its contact (dashed line) with a large bioherm in the middle part of the section; (g) detailed contact (dashed line) between stromatolites and granular limestones in the upper part of the section; (h) structural-textural features of the coarse-grained intraclastic limestones; (i) small stromatolite bioherm (outlined by dashed line) inside the packet of granular limestones in the lower part of the section.

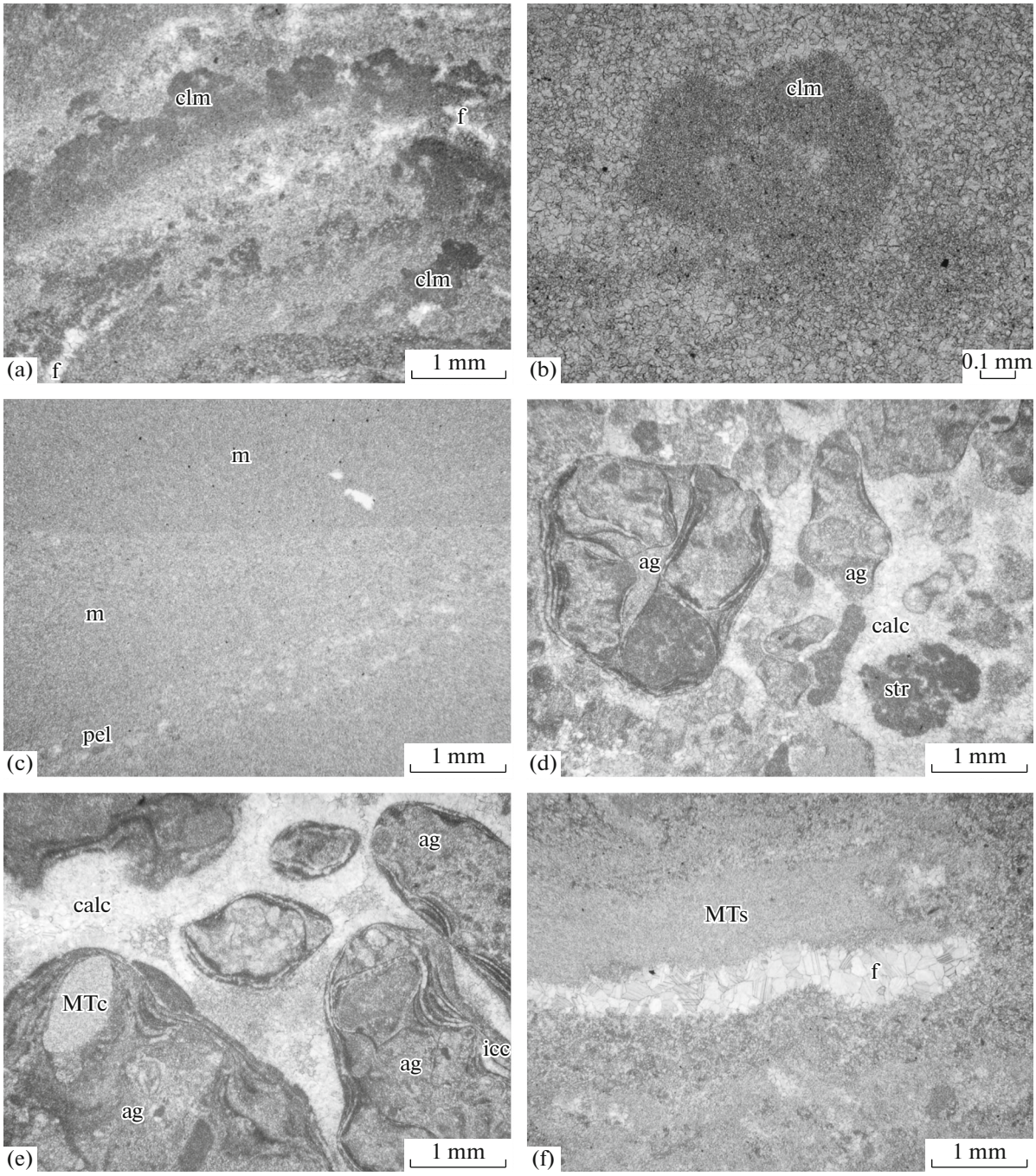

Fig. 5. Lithological characteristics of rocks of the Medved I member in thin sections. (a, b) Laminated bindstones and calcimicrobial boundstones of the stromatolitic column *Linella* inclined to the normal: intercalation of the micro- and cryptocrystalline varieties; calcimicrobes resemble renalcids; their clusters and orientation govern the general morphology of stromatolite laminae and the direction of column growth; and fenestra are also seen (sample 18.18-3-2); (c) layered calcimudstones in the interbioherm infill: homogeneous micrograined calcite dominates; some layers are represented by intraclastic-peloidal wackestones; and angle between the upper and lower bedding surfaces is prominent (sample 18.18-3-9); (d, e) intraclastic packstones and rudstones of layered packets; aggregate grains contain MT crack fragments, peloids, peloidal packstones or other aggregate grains (stromatoclasts are not usually detected inside aggregate grains); the grains are marked by poor sorting and different orientations; the cement/matrix ratio varies even within a single thin section: (d) sample 18.18-3-5, (e) sample 18.18-3-5a; (f) fine-grained peloidal wackestones with MT cracks (sample 18.18-3-3). (ag) Aggregate grains, (calc) calcite cement, (clm) calcimicrobes, (crc) "crystalloclasts," (dol) dolomite, (f) fenestra, (icc) isopachous calcite cement, (m) micrite, (MTc) fragments of MT cracks, (MTs) MT structures in situ, (pel) peloids, (si) silica concretions, (str) stromatoclasts.

The granular limestone packets are characterized by a cyclic pattern that is not always prominent. The bottom of cyclites is uneven, with erosion traces in some places. The coarse-grained varieties are confined usually to the lower parts of cyclites, whereas the middle part is composed of the finer-grained rocks of specific structures (with differently oriented cross-wavy bedding) and crosscut by intricate MT cracks (Fig. 5f). Small ripple marks are observed in the microgranular rocks in the upper parts of cyclites. The middle and upper elements of cyclites are often missing. Thickness of cyclites is variable but commonly not more than 1 m. In some places, the granular limestone packets contain small bioherms up to 40 cm high and 1 m long (Fig. 4i). Boundaries between the bioherms and granular limestone packets are distinct in most cases.

The granular limestone packets are exposed over a limited area along the lateral direction and traced only along the sublatitudinal direction over a few meters. They were likely extended along the submeridional direction or characterized by an intricate morphology.

Manaysu Member

In general, this member is lenticular-layered and characterized by an appreciable diversity of microfacies and lithotypes (Figs. 6, 7). Lithological properties of rocks lying at the same level, relative to the Medved I member top, change appreciably over a few tens of meters, probably, due to an irregular seafloor relief at the top of a huge stromatolite buildup and the consequent dissimilar sedimentation depth. Upward the section, the rocks become lithologically more consistent.

In the eastern part of the studied profile, stromatolitic bioherms in the Medved I member are overlapped by the micrograined argillaceous–carbonate rocks with specific loaf-shaped structures (Fig. 6a) resembling a coarse lenticular bedding or lens-shaped concretions. Upward the section, the member is marked by the appearance of limestone beds with the sand- and gravel-sized clasts (Fig. 7a) and a gradual increase of MT cracks (Fig. 7b). Westward, rocks overlying the stromatolitic bioherms become more diverse: in addition to the fine-grained limestones with numerous MT cracks, the coarse-grained varieties are also developed here (Fig. 2d). Moreover, one can see a lenticular stromatolitic limestone bed (about 2 m thick) overlain by poorly sorted clastic rocks (Fig. 6b). Rocks underlying this stromatolite bed (Fig. 2d) can be considered a transitional unit between the locally developed layered limestones of the underlying strata and the normal-layered rocks of the Manaysu member.

At some intervals, the member is characterized by a prominent cyclic structure (Figs. 6c, 6d). Average thickness of cyclites is about 15–20 cm, but some of their elements are appreciably thicker. The complete elementary cyclite commonly comprises three elements: lower element with different size of grains; middle element composed of not coarse well-sorted material and with differently oriented intricate MT cracks; and upper element composed of the finest-grained material with mainly bedding-perpendicular MT cracks. In some places, the cyclite bottom is marked by gutter casts (Fig. 6e). The MT clasts are abundant in the lower elements of cyclites. The shape and distribution of such clasts suggest their redeposition in the immediate vicinity of the crack formation site (Fig. 7c). In these coarse-grained rocks, the MT carbonate can also play the role of matrix (Fig. 7d). The middle element of cyclites is often characterized by the hummocky cross-stratification complicated by local deformations of the layer, and the bedding-parallel MT cracks emphasize the primary structure of rocks (Fig. 6f).

The member includes thin (<1 m) cross-layered calcarenite units (Fig. 6g), with the very fine- to fine-grained peloidal packstones and wackestones in some places and a large amount of subrounded clasts composed of the early diagenetic sparitic calcite cement (Fig. 7e). The coarser-grained calcarenites are intraclastic grainstones (ranging to rudstones) with the fine-crystalline mosaic cement. Allochems are represented by the aggregate grains composed of clasts of this cement mass ("crystalloclasts") as well (Fig. 7f). In general, such rocks are not very widespread but important for understanding the depositional environment of the sequence.

The Manaysu member is characterized by intense dolomitization and weak silicification. The sorted sandy and silty rocks (i.e., middle elements of cyclites) underwent high degree of dolomitization, but it did not affect the microsparite in MT structures.

The upper part of the member (~11 m) is almost completely composed of intraclastic varieties (Fig. 6h) subjected to intense postsedimentary transformation (recrystallization), similarly as the *Medved II member* (Fig. 8).

DISCUSSION

Morphology of Late Riphean Carbonate Platforms and Organogenic Buildups

In the Late Riphean, the BA region represented the proximal part of a passive margin of the East European Platform (Baltica/Rodinia shelf) (Maslov et al., 2002; Raaben, 2007), with an oceanic basin on the eastern side (in modern coordinates) (Li et al., 2013). Such environments (and geological bodies formed therein) with very low gradient (<1°) of the basin floor are called "carbonate ramps" and considered as a type of carbonate platforms (Ahr, 1973; Read, 1985). Processes of sediment deposition on carbonate ramps are influenced appreciably by transgressions and regressions, since even low-amplitude variations of the rela-

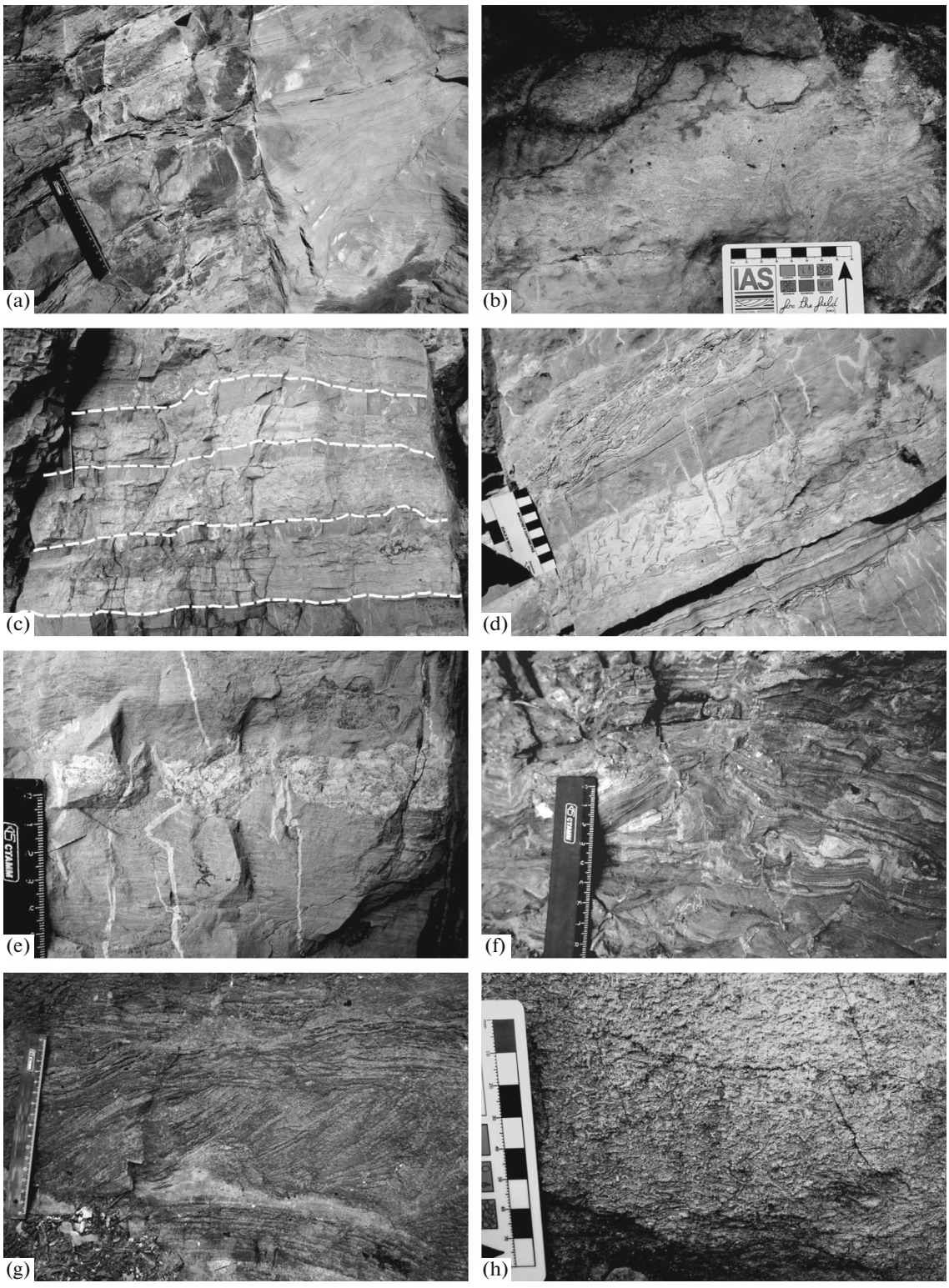

Fig. 6. Lithological characteristics of rocks of the Manaysu member. (a) Micrograined argillaceous–carbonate rocks at the bottom with lenticular structures; (b) coarse-clastic rocks immediately overlying the stromatolite bed in the lower part of the section; (c) cyclic sequence inside the Manaysu member (boundaries of elementary cyclites are shown by dashed lines); (d) various types of MT structures confined to different elements inside cyclites (see the text for explanation); (e) gutter casts at the base of an almost completely eroded cyclite; (f) hummocky cross-stratification complicated by plastic deformations (convolution?) and numerous differently oriented MT cracks; (g) cross-bedded calcarenites at one of the levels inside the member; (h) recrystallized intraclastic carbonates making up the upper part of the Manaysu member.

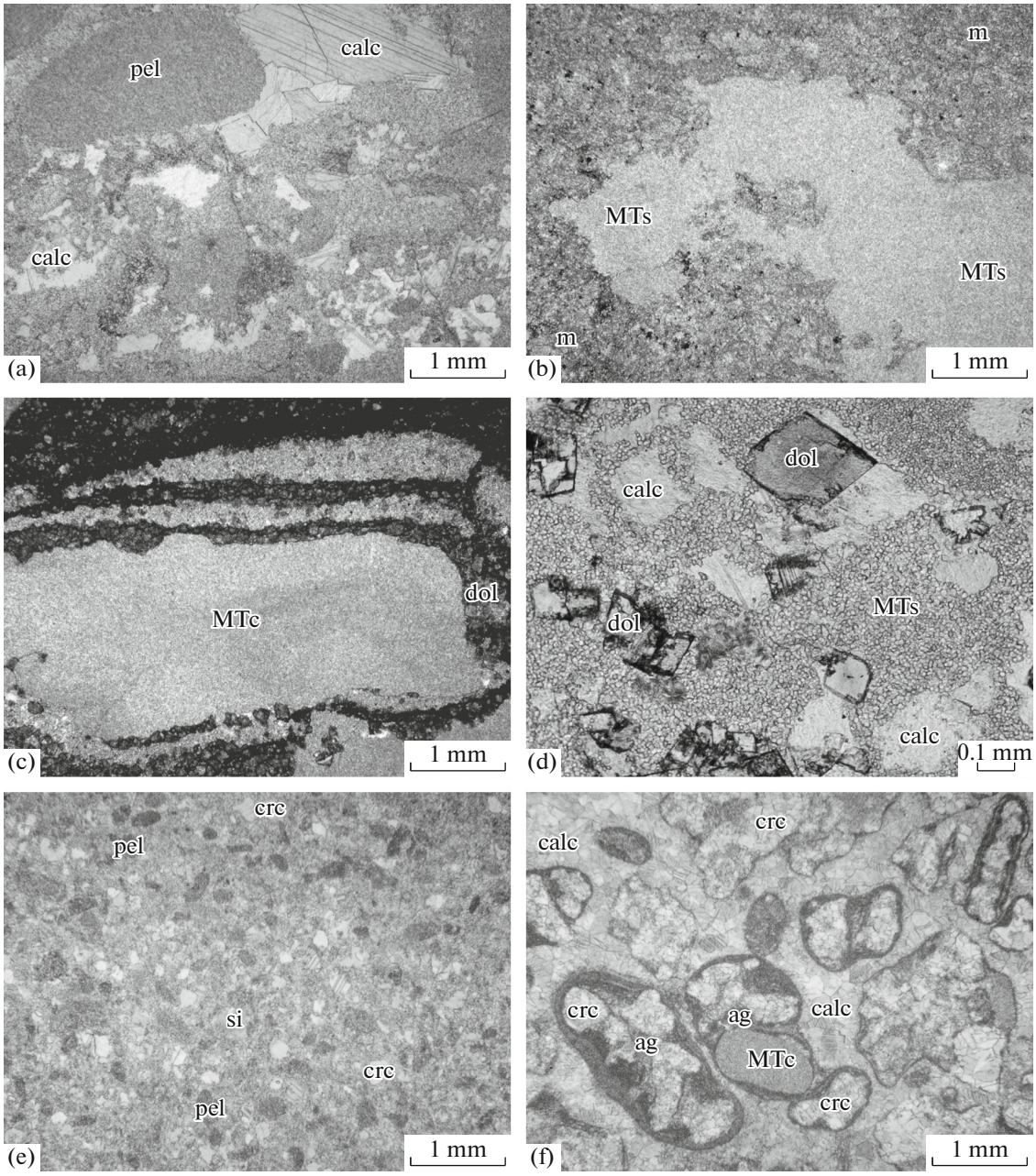

Fig. 7. Lithological characteristrics of rocks in the Manaysu member in thin sections. (a) Intraclastic packstone (sample 18.18-4-8) (the intergranular space contains the sparitic cement; the MT carbonate serves as the groundmass); (b) autochthonous MT structures in the micro- and fine-grained dolomitized rocks (sample 18.18-4-6); (c) MT clasts associated with the autochthonous MT cracks surrounded by the dolomitized groundmass (sample 18.18-4-9); (d) intergranular components of the intraclastic rudstones: MT carbonate, sparitic calcite, nearly euhedral dolomite (sample 18.18-4-11); (e) "crystalloclastic"-peloidal wackstone with silicified patches (sample 18.18-1-2); (f) intraclastic grainstone from the coarsest varieties of the cross-bedded calcarenites (sample 18.18-1-5). The remaining legend as in Fig. 5.

tive sea level induce a considerable lateral migration of facies belts (Bertrand-Sarfati and Moussine-Pouchkine, 1988; Burchette and Wright, 1992). If reef assemblages are developed, carbonate ramps can gradually be transformed into rimmed shelves (carbonate platforms with a subhorizontal floor surface in back-reef zones and steep slopes in the fore-reef zones) (Barnaby and Read, 1990).

In the Archean, Paleo- and Mesoproterozoic, stromatolites could likely make up real reefs (Allwood et al., 2006; Hoffman, 1989; Khabarov, 1999; and others) that served as a carbonate platforms rim and bor-

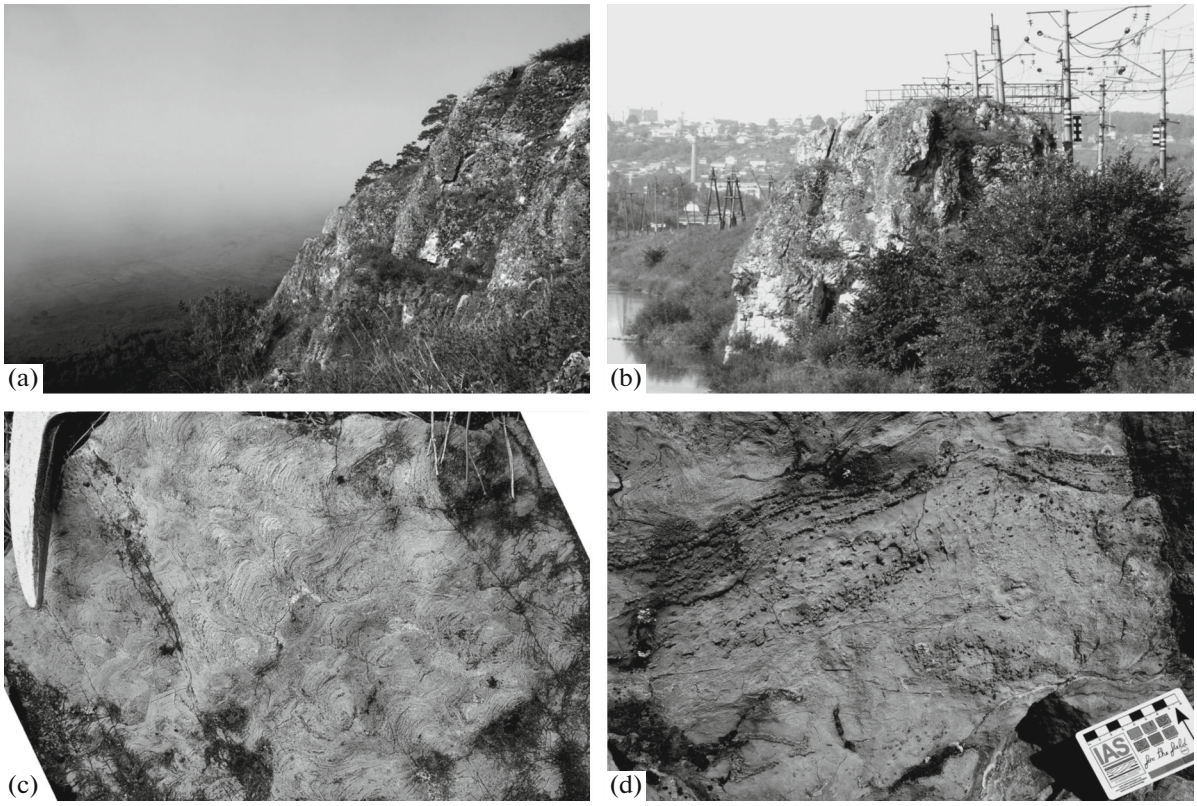

Fig. 8. Lithological characteristics of Medved II rocks. (a) General view of the upper part of the section (Manaysu and Medved II members); (b) outlier composed of stromatolites *Linella* located in the upper part of the Uk Formation section overlapped by rocks of the Bakeevo Formation; (c) *Linella*-bearing stromatolitic limestones altered by secondary processes; (d) granular rocks with different-size clasts and scattered silicification patches observed in some places within the stromatolite bioherm in the Medved II member.

der with open marine basins. However, decrease of the carbon dioxide concentration in the Early Neoproterozoic seawater provoked crisis in the stromatolitic reef formation because of attenuation of the role of chemogenic factor in the lithification of columns and retardation of the stromatolite growth rate (Grotzinger, 1990; Riding, 2011b). Therefore, Neoproterozoic carbonate platforms are represented mainly by ramps (Grotzinger and James, 2000), and stromatolite reefs are very scarce in the Tonian (Narbonne et al., 2000; Thorie et al., 2020; Turner et al., 2000). However, the Tonian is a period of the distribution of calcimicrobial (trombolite) buildups formed on the outer ramps. As real reefs, such buildups are marked by a prominent relief and clastic aprons (Batten et al., 2004; Turner et al., 1997). According to (Thorie et al., 2020), only one example of the Tonian rimmed shelf is known, whereas such geological structures are more widespread in the Cryogenian and Ediacaran. Hence, "stromatolitic meadows" (wide belts of organogenic buildups without contrast relief) were more typical for the Late Riphean carbonate platforms.

Modern marine stromatolites are detected mainly within the intertidal, upper subtidal, and, to a less extent, supratidal zones (Dill et al., 1986; Jahnert and Collins, 2012; Smith et al., 2018; and others) under extreme (for invertebrate animals) environments (Elliott, 1994; Garrett, 1970). Such environments, however, could previously be confined to a wider range of environment: the geological record includes examples of columnar stromatolites formed in much deeper waters (Bertrand-Sarfati and Moussine-Pouchkine, 1988; George, 1999; Monty, 1971). Possibility of a relatively deep-water genesis of many Precambrian and Phanerozoic stromatolites was suggested by the prominent Soviet paleontologists I. Krylov (1975) and S. Serebryakov (1975) almost half a century ago. Therefore, the principle of actualism turns out to be hardly suitable for reconstructing Neoproterozoic environments.

Composition of the Stromatolite-Forming Biota, Microstructures, and Shape of Stromatolites

Factors determining the shape of stromatolite columns and buildups remain a highly debatable issue (Awramik and Semikhatov, 1979; Dupraz et al., 2006; Golubic, 1991). Generally, the discussion is focused on the examination of two agents–hydrodynamics in the depositional environment and composition of the

stromatolite-forming biota. So far, it is impossible to define reliably the main factor governing the morphology of any stromatolite buildups in the geological past.

Microbial mats making up modern stromatolites include both filamentary and coccoid cyanobacteria, with the latter variety dominating in the columnar stromatolites (Jahnert and Collins, 2012; Suosaari et al., 2016). As noted by V. Maslov (1960), their ancient analogs lack such forms, but preservation of the morphology of cyanobacteria cells in stromatolites is promoted in some cases by the early diagenetic silicification (Golubic and Seong-Joo, 1999; Schopf, 2012). Alternation of the pelitomorphic and microcrystalline laminae manifested in stromatolites *Linella* is likely a primary feature unrelated with the process of irregular recrystallization, since such interlayering is repeated regularly in all columns.

Thus, the certain prevalence of crypto- and microcrystalline carbonates in columns is the most prominent microstructural feature of stromatolites *Linella*. The sparitic calcite is confined mainly to scarce fenestra, whereas allochems (mat-entrapped silt or sand-sized carbonate clasts) are commonly missing. Hence, we can make the following conclusions: (1) the formation of stromatolites was governed mainly by the microbial-induced mineralization; (2) input of the relatively coarse material in the stromatolite formation zone was extremely limited. It has been established that the Proterozoic was marked by a gradual decrease of the chemogenic (sparry crust) carbonates in stromatolites and the simultaneous increase of the micrograined component produced by the vital activity of cyanobacteria. Therefore, the "micrite-forming" or fine-grained stromatolites are most typical for the Neoproterozoic (Grotzinger and Knoll, 1999; Riding, 2011b). Probably, herein lies the main genetic distinction of the Neoproterozoic stromatolites from some similar ones in Mesoproterozoic, described, e.g., in (Tosti and Riding, 2017), where the fine-grained carbonate was accumulated due to the agglutination of water-suspended particulates by the microbial mat. It is also shown that the branching ability of some Neoproterozoic (850–750 Ma interval) stromatolites can be suppressed by an intense input of carbonate clasts (Planavsky and Grey, 2008)[1]. Interpolating this trend onto the actively branching stromatolites *Linella*, one can assume that development of the latter stromatolites can also be related to induced biomineralization under a deficit of the mechanogenic material.

The following fact deserves special discussion: the stromatolites include well-preserved cluster calcimicrobes of *Renalcis*-type. This feature was mentioned by I. Krylov (1967) who described the genus *Linella* for the first time, but did not provide the interpretation. The revealed textures do not associate with diagenetic alterations and are unrelated to the development of stylolitic sutures, but they were certainly present in ancient microbial mats. They are really calcimicrobes and unrelated to random deformations of the weakly lithified mats–this fact is supported by their regular laminae-perpendicular orientation in columns.

It is believed that calcimicrobes appeared in the geological record in the Mesoproterozoic (Kah and Riding, 2007). In the Neoproterozoic, they could make up autonomous organogenic buildups (similar to the Phanerozoic mud mounds) in relatively deep waters (Aitken, 1967; Batten et al., 2004; Turner et al., 1997).

Given that the nonlayered sectors of calcimicrobial boundstones in columns are interpreted as trombolites, the Uk stromatolites should be considered as trombolite-stromatolite structures (or calcimicrobial stromatolites). Findings of calcimicrobes in the Precambrian stromatolites are known at present (Riding, 2011a; Turner et al., 2000). However, calcimicrobes in the Uk Formation differ from the real *Renalcis* by the absence of an explicit internal cavity.

Remains of *Renalcis* sensu stricto are considered problematic, because their modern analogs are lacking. We do not even know whether they are prokaryotes or eukaryotes. Most commonly, they are identified as calcareous cyanobacteria (Riding, 2011a). According to A. Zhuravlev, renalcids should be assigned neither to the calcareous algae nor to cyanobacteria, and their microstructure is similar to that of some sponges and cnidarians (Zhuravlev, 2001, 2013). It is believed that this taxa only appeared in the end-Vendian, and the older remains lack the specific microstructure and "skeleton" (Zhuravlev, 2001).

The obtained data on the composition of biomarkers in the Upper Uk Subformation rocks indicate unambiguously the eukaryotic communities existence in the sedimentary basin (Maslov et al., 2019). Probably, the calcimicrobial microstructures observed in stromatolites *Linella* belong to eucaryotes. Compared with the spatial orientation of columns, analysis of stromatolites in thin sections shows that the column growth strategy was governed precisely by these organisms (most probably, photosynthesizers).

MT Structures and Depositional Environments

The MT cracks are early diagenetic banded, vermicular, spindle-shaped or filamentary structures composed of the uniform equant microspar. They represent a major component of Proterozoic deposits (James et al., 1998; Kuang, 2014; Kuznetsov, 2005; Pollock et al., 2006). Such structures show a rigorous stratigraphic constraint (2600–717 Ma). With a few exceptions,[2] they are missing in rocks younger than the

[1] More precisely, reduction of the allochem input volume enhanced the role of autochthonous accumulation of the micritic carbonate and initiation of the branching of stromatolites.

[2] They represent cap carbonates of the Marino Glaciation in Namibia and one of the layers in the Ediacaran sequence in Australia.

Cryogenian (Bishop and Sumner, 2006; Hodgskiss et al., 2018; Shields, 2002). Though most widespread in rocks of the tidal and subtidal zones, they are much rarer within the lower (below the storm wave base)[3] and supratidal zones (Kuang, 2014). Despite a vast number of versions explaining the origin of MT cracks (Petrov, 2011; Pratt, 1998; Smith, 2016), it is notable that such structures are assigned commonly to carbonates containing the clay material admixture (Hodgskiss et al., 2018).

In the Uk Formation, MT structures are most widespread in the upper part of the Lower Subformation and in the Manaysu member of the Upper Subformation. In the Medved I member, they are very rare and only confined to some levels within the granular limestone packets. It is important that MT cracks are missing in stromatolite bioherms *Linella*, although examples of stromatolites complicated by such cracks are known in the geological record (Kuang, 2014; Petrov, 2011, p. 12). Such structures are also absent in the interbiohermal lenses of micrograined sediments, although the terrigenous mud is present in them. Probably, this fact suggests the other geochemical environments for the granular deposits generation. The amount of MT structures is fundamentally different in two adjacent members (Medved and Manaysu), suggesting a distinct difference in depths of their formation.

The lower part of the Manaysu member is characterized mainly by the abundance and diversity of MT structures. Among them, one can see both autochthonous and allochthonous structures, indicating a permanent reworking of sediments. Probably, the redeposition was provided primarily by storm activity, because MT structures in the Uk Formation are associated mainly with cyclic tempestites. Since cyclites are lithologically heterogeneous (because of variable hydrodynamics), MT cracks confined to different elements of cyclites also differ from each other in shape and represent specific hydrodynamic setting indicators: subnormal cracks suggest a passive or moderate depositional environment, whereas the bedding-conformal or irregular cracks indicate that the environment was more active but weaker than the environment during the seafloor erosion and the MT clast formation.

Storm Sedimentation on Carbonate Ramps

Depending on the hydrodynamics, any carbonate ramp can be divided into three parts: inner, middle, and outer. The upper boundary of the middle ramp is defined by the normal wave base; the lower boundary, by the storm wave base irrespective of the absolute depth mark of basin (Burchette and Wright, 1992). Ramps are subjected to the influence of tidal, wave, and storm activities. In particular, ramps dominated by the storm sedimentation are typical for the Neoproterozoic (Grotzinger and James, 2000).

The formation of storm deposits (tempestites) is attributed to both oscillatory and unidirectional movements of water masses, whereas the latter can be expressed as geostrophic and density (hyperpycnal) flows (Myrow, 1992; Myrow and Southard, 1996; Seilacher and Aigner, 1991). These deposits are marked by the hummocky cross-stratification. The presence of gutter casts, amalgamation of cyclites, and areal distribution of storm layers can be controlled by the shallow-water facies (Einsele and Seilacher, 1991). The erosional bottom of cyclites and the gradational sorting of material make these rocks similar to other event deposits (first of all, turbidites). Both types of deposits can be characterized by ripple marks (generated by waves and currents) and plastic (soft-sediment) deformation structures including the convolute bedding in the middle part of cyclites (Chen and Lee, 2013; Einsele and Seilacher, 1991; Molina et al., 1998).

Traditionally, proximal and distal tempestites are recognized: increase of depth is correlating with growing volume of fine-grained material, thinning of cyclites, and decrease of erosion marks amount at the base (Einsele, 2000; Seilacher and Aigner, 1991). It was shown recently that such model can be applied to a relatively steep slope, whereas the low-gradient ramps are characterized by a more complicated distribution of tempestites (Jelby et al., 2020).

Researchers believe that the hummocky cross-stratification is related to storm activity (Einsele, 2000; Jelby et al., 2020; Myrow, 1992; Seilacher and Aigner, 1991; Swift et al., 1983; and others). According to (Dumas and Arnott, 2006), such sedimentary structure indicates a depth interval between the normal and storm wave bases. However, some works suggest that sediments with this type of bedding can also be deposited in the shallower-water environment within the tidal activity zone (Basilici et al., 2012; Yang et al., 2005). Moreover, signs of such activity are not always identified easily in sediments of ramps (Vakarelov et al., 2012). It is already proved now that the hummocky cross-stratification is polygenous and can hardly serve as an adequate indicator of the basin depth (Jelby et al., 2020 and references therein).

In the Upper Uk Subformation, rocks with signs of storm genesis are observed in the Medved I and Manaysu members. The Medved I member contains two fundamentally different lithotypes influenced by the storm activity to different extent: packets of intraclastic layered limestones and interbiohermal micrograined rocks. The formation of the first variety was likely caused by unidirectional migrations of water masses; the second is related to oscillatory movements in the depositional environment. In contrast, tempestites in the Manaysu member are characterized by the lateral extension and prominent cyclicity.

[3] Some authors, e.g., Purkis et al. (2015), relate the upper/lower subtidal (more precisely, shallow- and deep-water subtidal) boundary to the normal wave base.

RESULTS OF THE DEPOSITIONAL ENVIRONMENT ANALYSIS

Yuryuzan Member

The Yuryuzan member formed near the coastal zones with a sufficiently active or moderate hydrodynamics, as suggested by the abundance of terrigenous admixture and relatively large (>2 mm) carbonate clasts in the intercolumn space of stromatolites (rudstones and packstones). According to (Kuang et al., 2019), thin-columnar and branching stromatolites similar to *Patomella* can be typical of the intertidal zones. Stromatolite buildups in the member, however, lack distinct signs of the subaerial exposure. At the same time, abundance of the terrigenous admixture can suggest proximity of the watercourse inflow into the marine basin. This assumption is supported by the detection of analogous stromatolites in the lower part of the Lower Uk Subformation in the Akkostyak section (*Stratotip* ..., 1983; our observations) in association with oolites and oncolites (i.e., at a lower stratigraphic level in undoubtedly shallow-water deposits). The Lower Uk stromatolites in the Akkostyak section is marked by the following fundamental distinction: stromatolitic columns are surrounded by the terrigenous material, while stromatolites *Patomella* in the Upper Uk (Yuryuzan) bioherms are hosted in the carbonate deposits.

The obtained data on modern stromatolites demonstrate that the oriented water flow produces not only elongated stromatolite columns but also isometric structures. In addition, strong current is suggested by a distinct intercolumn space (Bosak et al., 2013). It is also known that the abundance of suspended particles in water column commonly suppresses the growth of stromatolites (Krylov, 1975). Thus, stromatolite buildups in the Yuryuzan member were formed likely at depths corresponding to the upper subtidal-peritidal zone, with some influence of currents generated by a stream (river arm?) flowing into the marine basin.

Medved I Member

The study of **stromatolite buildups** in the Medved I member revealed that they did not belong to the tidal zone, because rocks here lack desiccation cracks, evidences of the presence of evaporites, oolites, teepee structures, and other typical littoral signatures (Eriksson and Simpson, 2011; Semeniuk, 2019), but the stromatolites often contain fenestra that are usually considered indicators of the subaerial environment (Flügel, 2010; Shinn, 1968). However, probably, this sole sign cannot serve as a strong argument for reconstructions, since fenestra are often associated with microbial mats (Gerdes, 2007), irrespective of facies.

In general, the presence of large columnar stromatolites is considered indicator of a large volume of accommodation space, as demonstrated with modern Bahamian microbialites as example (Andres and Reid, 2006). Macroscopic observations of the Ust-Katav section revealed that stromatolites in the Medved member "tended" to occupy completely the surrounding space during the growth, possibly, because of rivalry of the adjacent colonies for the access to light. Evidently, they formed under stable conditions at depths allowing free growth and lacking significant obstructions (wave-swash activity or water level fall).

It is believed that lowering of the hydrodynamic level should lead to decrease in the diameter of stromatolite columns (Bosak et al., 2013; Dupraz et al., 2006). Such trend, however, is maintained not always, because, in addition to hydrodynamics, rates of the sedimentation and basin floor subsidence can also influence the stromatolite morphology (Serebryakov, 1975). For example, the Uk Formation shows a relative upsection decrease of the intercolumn space in stromatolite bioherms, suggesting the transition to a calmer water environment due to the basin deepening. This trend is also indicated by a substantial decrease of the terrigenous sandy–silty admixture in bioherms *Linella* relative to bioherms *Patomella*.

Microfacies of the **interbiohermal infill** suggest a low mobility of the depositional environment. Another significant facies indicator is represented by specific sedimentary structures of these rocks: some cross-sections are dominated by the hummocky (but small-scale) cross-stratification owing to storm activity (Dumas and Arnott, 2006; Jelby et al., 2020; Swift et al., 1983). Undoubtedly, such micrograined rocks with signs of the storm impact could only accumulate in the normal wave-protected zones, probably, below NWB. Probably, they represent suspended sediments deposited in cavities inside the organogenic buildups.

An essential information is obtained from the detailed lithofacies analysis of the **packets of layered limestones** represented mainly by intraclast varieties. Note that limestones in such packets were described as "microphytolites" in previous works (Kozlov, 1982; *Stratotip* ..., 1982). A major part of intraclasts comprises aggregate grains of different genesis. By analogy with the modern Bahamian grapestones, we can assume that such morphological elements are formed in an environment with moderate wave hydrodynamics (Gischler, 2011)[4]. Evidently, the grains were redeposited several times until their burial at depths below the normal wave base. At the same time, stromatolite clasts in the granular limestones lack signs of reworking. Therefore, they should be considered as "local" material entrapped by the flow evacuating fragments of the peloidal packstones and MT cracks (primary components of aggregate grains) from the shallower water zones to deep zones. Many grains are surrounded by a crustification rim—early diagenetic

[4] Analogy here can only be approximate, because modern grapestones are also formed with an active participation of green algae that stabilize and micritize the sediment (*Carbonate* ..., 1972 and others).

marine phreatic cement typical for the upper subtidal environment (Grammer et al., 1999; Hosa and Wood, 2017). In addition, oolites (typical of the mobile shallow-water environment) are absent among the allochems. In general, judging from the nature of clasts, they were delivered mainly from relatively calm-water sediments in the inner ramp.

These sediments were accumulated synchronously with the growth of buildups but in a pulsed manner, as suggested by the cyclic structure of packets, gradational sorting of material in some beds, and rare erosional marks at the bottom. In addition, granular limestone packets lack signs of the wave reworking. Assumption about the event sedimentation is supported by the findings of small stromatolite bioherms within the layered packets. According to this scenario, sediments were subjected to rapid lithification. Therefore, the mechanogenic sediments served as a sufficiently stable substrate for colonization by the stromatolite-forming biota. Early cementation was also responsible for a scarcity of gutters at the bottom of cyclites. In the middle or upper elements of cyclites, MT structures are observed in some places, making these sediments similar to cyclites in the overlying Manaysu member.

Genetic fingerprints of these cyclites are typical for both tempestites and turbidites, according to (Einsele and Seilacher, 1991). On the one hand, layered packets are mainly composed of the allochthonous (relative to the surrounding deposits) material, serving as argument in favor of their assignment to the latter category. On the other hand, this material is sorted not very well, and the cyclites lack explicit succession of elements typical for the Bouma Cycle. Most probably, layered limestone packets represent the sedimentary infill of channels passing the periodic flows—water masses induced by storms in the shoal zone, resulting in erosion of the seafloor and unloading of sediments at the return to deep zone. Such sedimentation model is characterized by the tempestites (Myrow, 1992). Configuration of the assumed north-to-south (in modern coordinates) oriented channels apparently contradicts the assumption of the west-to-east material transport in the Late Riphean (from the shallow-water zone to open sea) (Maslov et al., 2002). However, according to (Einsele, 2000; Myrow and Southard, 1996; Swift et al., 1983), modern storm-induced geostrophic currents can deviate toward the meridional direction because of the Coriolis force.

Most probably, carbonate breccias, as well as calcarenite sheets with the signs of wave hydrodynamics, are not typical for the Medved I member. Therefore, organogenic stromatolite buildups probably lacked a high positive relief (typical of reefs sensu stricto). Hence, the carbonate platform represents a ramp but not rimmed shelf. At the same time, the Medved I member is characterized by a rather great thickness. Evidently, the long-term, relatively stable sedimentology in a large epiplatform basin could only be guaranteed by sufficient depths. Otherwise, sea level fluctuations should be fixed somehow in the geological record. Hence, stromatolite "meadows" formed below the normal wave base (middle part of ramp or deeper) within the photic zone (extending to a depth of several decameters) are characterized by a deficit of the clastic material and a slow sea level rise. At the same time, such a facies belt was complicated by channels filled with sediments during storms.

Manaysu Member

We analyzed structures and textures of rocks, as well as the available general geological data, and identified facies nature of this member.

In contrast to intraclastic limestones in the Medved I member, the cyclic architecture of rocks in the Manaysu member are traced along the lateral direction. They comprised by "local" clasts with occasional signs of the hummocky cross-stratification in combination with plastic deformation structures, making it possible to define them as tempestites. A small share of micrograined sediments in them and sufficient abundance of gutter casts at the bottom indicate that they, probably, are not distal varieties. In addition, the member includes micrograined argillaceous limestones with specific lenticular structures (typical of rocks lying immediately above the stromatolite buildups) that are also produced by storm activity but, probably, in relatively deeper zones.

The member includes not only deposits related to storm waves, but also sediments deposited in the normal wave zone (cross-bedded calcarenites in the middle lower part of the member, as well as intensely altered intraclastic limestones at upper intervals). Therefore, we assume that sedimentation at this time took place near the normal wave base, within the upper part of the middle ramp and the lower part of the inner ramp. One cannot rule out, however, that some volume of sediments was deposited within the peritidal zone, but reliable confirmations are missing—tidal processes within the carbonate ramps can be camouflaged by the wave or storm activity (Vakarelov et al., 2012).

Rocks of the Manaysu member contain carbonate "crystalloclasts"—clasts of the early diagenetic marine cement composed of separate crystals or their aggregates. The calcarenites include the mosaic calcite cement with subeuhedral crystals. According to E. Flügel (2010), the cement with such spatial characteristics are formed both during the burial of sedimentary sequences and during the initial postsedimentary stages with the participation of meteogenic waters. Since relation with the early diagenetic processes is obvious in this case, we should admit that the formation of calcarenites could be fostered by an extremely shallow-water environment.

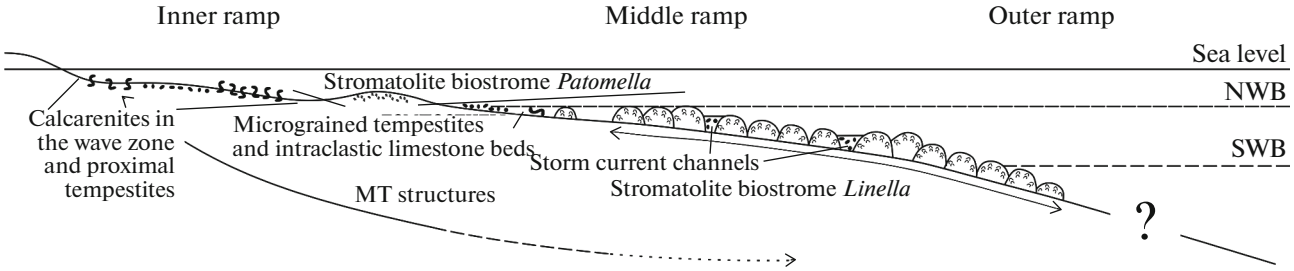

Fig. 9. Schematic profile of the carbonate ramp during the deposition of the Upper Uk Subformation sediments. (NWB) normal wave base, (SWB) storm wave base.

The entire upper part of the member comprises intraclastic rocks composed mainly of aggregate grains. By analogy with modern grapestones, we can suppose somewhat conventionally a rather shallow-water environment protected from the active wave hydrodynamics.

The mosaic facies pattern observed in the Manaysu member is consistent with the assumed shallow-water

Table 1. Microfacies, lithotypes, genetic types, and facies typical for the Upper Uk Subformation section

Member	Microfacies	Lithotypes (microfacies types)	Genetic types	Facies
Yuryuzan	Laminated bindstones	Thin-columnar stromatolitic boundstones – stromatolites *Patomella*	Stromatolite build-ups/bioherms?	Proximal organogenic buildups
	Intraclastic packstones	Intraclastic intercolumn deposits		
	Intraclastic rudstones			
Medved	Laminated bindstones	Thick-columnar stromatolitic boundstones – stromatolites *Linella*	Stromatolitic bioherms	Distal organogenic buildups (middle ramp)
	Nonlayered fenestral and calcimicrobial boundstones			
	Calcimudstones	Fine- to micrograined limestones, sometimes argillaceous	Interbiohermal suspended deposits	
	Intraclastic-peloidal wackestones			
	Fenestral bindstones			
	Intraclastic packstones	Intraclastic limestones/calcarenites, rarely with MT cracks	Channel tempestites/storm turbidites	Infill of storm (geostrophic) current channels
	Intraclastic rudstones			
	Intraclastic grainstones			
	Peloidal wackestones (?) with MT cracks			
	Microlayered calcimudstones or bindstones	Micrograined limestones	Suspended deposits	
Manaysu	Intraclastic rudstones with MT clasts	Intraclastic coarse-grained limestones with MT clasts (lower elements of cyclites)	Proximal tempestites	Deposits in the inner ramp or upper part of the middle ramp
	Intraclastic packstones with MT clasts			
	Intraclastic packstones with MT cracks	Intraclastic fine-grained limestones with MT cracks (middle element of cyclites)		
	Intraclastic wackestones with MT cracks			
	Calcimudstones with MT cracks	Micrograined limestones with MT cracks (upper element of cyclites)		
	“Crystalloclastic”-peloidal packstones	Calcarenites, sometimes with cross-bedding	Shallow-water (agitation zone) deposits	
	“Crystalloclastic”-peloidal wackestones			
	Intraclastic grainstones			

depositional environment. Based on the example of modern shelf basins, Purkis et al. (2015) demonstrated convincingly that depths less than 40 m are characterized by a very wide range of lithotypes and facies. Distribution of storm deposits in the shoal zone supports the conclusion about the lack of reef rim in the carbonate platform. A gradual deepening of the basin is indicated by the facies homogeneity in the upper part of the Manaysu member.

CONCLUSIONS

The model based on a detailed lithofacies analysis of the sedimentary system in the Upper Uk Subformation is generally consistent with the earlier versions proposed for Proterozoic carbonate platforms in other regions (Bertrand-Sarfati and Moussine-Pouchkine, 1988; James et al., 1998; Khabarov, 1999; Petrov and Semikhatov, 2009). Data on the facies distribution is presented in the general form in Table 1, schematic profile of the carbonate ramp is shown in Fig. 9.

In general, the successive grading of coastal-marine deposits of the Lower Uk Subformation into the moderately shallow-water (Yuryuzan member) and relatively deep-water (Medved I member) deposits fits the transgressive trend of the South Ural basin evolution in the middle Neoproterozoic. The subsequent appreciable attenuation of the sea level rise (or its lowering) provoked a drastic facies change and formation of the shallow-water Manaysu member. It is dominated by deposits of the inner–upper middle ramp with traces of storm impact, as well as wave reworking at some intervals. One cannot also rule out the influence of tidal processes. Replacement of intraclastic limestones in the upper part of the Manaysu member by stromatolite buildups in the Medved II member reflects a new transgressive trend. It is difficult to infer steepness of the carbonate ramp and scenario of the basin depth variation (or other conditions) required for the termination or resumption of the stromatolite buildup growth.

The upper boundary of the Uk Formation corresponds to a great hiatus in the geological record associated with the onset of planetary glaciations. Undoubtedly, this hiatus was accompanied by the erosion of sedimentary strata in the upper part of the Karatau Group, resulting in absence of the Uk Formation in several areas of BA.

ACKNOWLEDGEMENTS

The authors are grateful to A.V. Maslov for assistance in research works, valuable advices, and critical remarks in the manuscript and to M.T. Krupenin for help in the study of the Akkostyak section. We also thank two anonymous peers and editors who made it possible to refine the manuscript.

FUNDING

This work was supported by the Russian Foundation for Basic Research, project no. 18-05-00062.

REFERENCES

Ahr, W.M., The carbonate ramp—an alternative to the shelf model, *Gulf Coast Ass. Geol. Soc. Trans.*, 1973, vol. 23, pp. 221–225.

Aitken, J.D., Classification and environmental significance of cryptalgal limestones and dolomites, with illustrations from the Cambrian and Ordovician of southwestern Alberta, *J. Sediment. Petrol.*, 1967, vol. 37, pp. 1163–1178.

Allwood, A.C., Walter, M.R., Kamber, B.S., et al., Stromatolite reef from the Early Archaean era of Australia, *Nature*, 2006, vol. 441, pp. 714–718.

Andres, M.S. and Reid, R.P., Growth morphologies of modern marine stromatolites: A case study from Highborne Cay, Bahamas, *Sediment. Geol.*, 2006, vol. 185, pp. 319–328.

Awramik, S.M. and Semikhatov, M.A., The relationship between morphology, microstructure, and microbiota in three vertically intergrading stromatolites from the Gunflint Iron Formation, *Can. J. Earth Sci.*, 1979, vol. 16, no. 3, pp. 484–495.

Barnaby, R.J. and Read, J.F., Carbonate ramp to rimmed shelf evolution: Lower to Middle Cambrian continental margin, Virginia Appalachians, *Geology*, 1990, vol. 102, pp. 391–404.

Basilici, G., de Luca, P.H.V., and Oliveira, P., A depositional model for a wave-dominated open-coast tidal flat, based on analyses of the Cambrian-Ordovician Lagarto and Palmares formations, north-eastern Brazil, *Sedimentology*, 2012, vol. 59, pp. 1613–1639.

Batten, K.L., Narbonne, G.M., and James, N.P., Paleoenvironments and growth of Early Neoproterozoic calcimicrobial reefs: platformal Little Dal Group, northwestern Canada, *Precambrian Res.*, 2004, vol. 133, no. 3/4, pp. 249–269.

Bekker, Yu.R., Age and succession of rocks in the upper part of the Karatau Group, southern Urals, *Izv. Akad. Nauk SSSR, Ser. Geol.*, 1961, no. 9, pp. 49–60.

Bertrand-Sarfati, J., Is cratonic sedimentation consistent with available models? An example from the Upper Proterozoic of the West Africa Craton, *Sediment. Geol.*, 1988, vol. 58, nos. 2/4, pp. 255–276.

Bishop, J.W. and Sumner, D.Y., Molar tooth structures of the Neoarchean Monteville Formation, Transvaal Supergroup, South Africa. I: Constraints on micro-crystalline $CaCO_3$ precipitation, *Sedimentology*, 2006, vol. 53, no. 5, pp. 1049–1068.

Bosak, T., Knoll, A.H., and Petroff, A.P., The meaning of stromatolites, *Ann. Rev. Earth Planet. Sci.*, 2013, vol. 41, pp. 21–44.

Burchette, T.P. and Wright, V.P., Carbonate ramp depositional systems, *Sediment. Geol.*, 1992, vol. 79, pp. 3–57.

Carbonate Sediments and Their Diagenesis, Bathurst, R.G.C., Ed., Amsterdam: Elsevier, 1972. Chen, J. and Lee, H.S., Soft-sediment deformation structures in Cambrian siliciclastic and carbonate storm deposits (Shandong Province, China): Differential liquefaction and fluidization triggered

by storm-wave loading, *Sediment. Geol.*, vol. 288, pp. 81–94.

Dill, R.F., Shinn, E.A., Jones, A.T., et al., Giant subtidal stromatolites forming in normal salinity waters, *Nature*, 1986, vol. 324, pp. 55–58.

Domrachev, S.M., Devonian in the Karatau Range and adjacent regions of the Southern Urals, in *Devon Zapadnogo Priural'ya* (Devonian in the Western Ural Region), Leningrad, 1952, pp. 5–121.

Dub, S.A. and Grazhdankin, D.V., Carbonate facies of the Upper Riphean Uk Formation in the Medved section (Shubino): An Overview, in *Materialy 3-ei Vserossiiskoi litologicheskoi shkoly* (Materials of the 3rd All-Russia Lithological School), Yekaterinburg, 2018, pp. 69–72.

Dub, S.A., Cherednichenko, N.V., Kiseleva, D.V., et al., Trace element behaviour in acidic leachates (acetic, nitric and hydrochloric) from siliciclastic-carbonate rocks of the Upper Riphean Uk formation in the Southern Urals, *Litosfera*, 2019, vol. 19, no. 6, pp. 919–944.

Dumas, S. and Arnott, R.W.C., Origin of hummocky and swaley cross-stratification—the controlling influence of unidirectional current strength and aggradation rate, *Geology*, 2006, vol. 34, pp. 1073–1076.

Dunham, R.J., Classification of carbonate rocks according to depositional texture, in *Classification of Carbonate Rocks*, Ham, W.E., Ed., *AAPG. Mem.*, 1962, vol. 1, pp. 108–121.

Dupraz, C., Pattisina, R., and Verrecchia, E.R., Translation of energy into morphology: simulation of stromatolite morphospace using a stochastic model, *Sediment. Geol.* 2006, vol. 185, pp. 185–203.

Einsele, G., *Sedimentary, Basins. Evolution, Facies, andSsediment Budget*, Berlin: Springer, 2000.

Einsele, G. and Seilacher, A., Distinction of tempestites and turbidites, in *Cycles and Events in Stratigraphy*, Einsele, G., Ricken, W., and Seilacher, A., Eds., Berlin: Springer, 1991, pp. 377–382.

Elliott, W.M., Stromatolites of the Bahamas, in The 26th Meet. Ass. Mar. Lab. Caribbean, San Salvador: Bahamian Field Station, 1994, p. 33–39.

Embry, A.F. and Klovan, J.E., A Late Devonian reef tract on Northeastern Banks Island, NWT, *Bull. Can. Petrol. Geol.*, 1971, vol. 19, pp. 730–781.

Eriksson, K.A. and Simpson, E., Precambrian tidal facies, in *Principles of Tidal Sedimentology*, Davis, R.A. and Darlymple, R.W., Eds., New York: Springer, 2011, pp. 397–419.

Flügel, E., *Microfacies of Carbonate Rocks. Analysis, Interpretation and Application*, Berlin: Springer, 2010.

Frolov, V.T., *Geneticheskaya tipizatsiya morskikh otlozhenii* (Genetic Typification of Marine Deposits), Moscow: Nedra, 1984.

Garrett, P., Phanerozoic stromatolites: noncompetitive ecologic restriction by grazing and burrowing animals, *Science*, 1970, vol. 169, pp. 171–173.

George, A.D., Deep-water stromatolites, Canning Basin, northwestern Australia, *Palaios*, 1999, vol. 14, pp. 493–505.

Gerdes, G., Structures left by modern microbial mats in their host sediments. in *Atlas of Microbial Mat Features Preserved within the Siliciclastic Rock Record. Atlases*, in *Geoscience 2*, Schieber, J., Bose, P.K., and Eriksson, P.G., Eds., Amsterdam: Elsevier, 2007, pp. 258–265.

Gischler, E., Carbonate environments, in *Encyclopedia of Geobiology. Encyclopedia of Earth Sciences Series*, Reitner, J. and Thiel, V., Eds., Dordrecht: Springer, 2011, pp. 238–260.

Golubic, S., Modern stromatolites—a review, in *Calcareous Algae and Stromatolites*, Riding, R., Ed., Berlin: Springer, 1991, pp. 541–561.

Golubic, S. and Seong-Joo, L., Early cyanobacterial fossil record: preservation, palaeoenvironments and identification, *Eur. J. Phycol.*, 1999, vol. 34, no. 4, pp. 339–348.

Gorozhanin, V.M., Michurin, S.V., Voikina, Z.A., et al., Marino–glacial deposits in the Tolparovo section of the upper Precambrian (Zilim and Malyi Tolpar rivers), *Geol. Vestn.*, 2019, no. 3, pp. 69–92.

Gosudarstvennaya geologicheskaya karta RF m-ba 1 : 1000000 (tret'e pokolenie). List N-40 (State Geological Map of the Russian Federation. Scale 1 : 1000000, Sheet N-40), St. Petersburg: Kartogr. Fabr. VSEGEI, 2013.

Grammer, G.M., Crescini, C.M., McNeill, D.F., and Taylor, L.H., Quantifying rates of syndepositional marine cementation in deeper platform environments-new insight into a fundamental process, *J. Sediment. Res.*, 1999, vol. 69, pp. 202–207.

Grotzinger, J.P., Geochemical model for Proterozoic stromatolite decline, *Am. J. Sci.*, 1990, vol. 290, pp. 80–103.

Grotzinger, J.P. and James, N.P., Precambrian carbonates: evolution of understanding, in *Carbonate Sedimentation and Diagenesis in the Evolving Precambrian World*, Grotzinger, J.P. and James, N.P., Eds., in *SEPM Spec. Publ.*, 2000, no. 67, pp. 3–22.

Grotzinger, J.P. and Knoll, A.H., Stromatolites in Precambrian carbonates: evolutionary mileposts or environmental dipsticks?, *Ann. Rev. Earth Planet. Sci.*, 1999, vol. 27, pp. 313–358.

Hodgskiss, M.S.W., Kunzmann, M., Poirier, A., and Halverson, G.P., The role of microbial iron reduction in the formation of Proterozoic molar tooth structures, *Earth Planet. Sci. Lett.*, 2018, vol. 482, pp. 1–11.

Hoffman, P.F., Pethei reef complex (1.9 Ga), Great Slave Lake, NWT, in *Reefs: Canada and Adjacent Areas (Can. Soc. Petrol. Geolog. Mem.)*, Geldsetzer, H.H.J., James, N.P., and Tebbutt, G.E., Eds., 1989, vol. 13, pp. 33–48.

Hosa, A. and Wood, R., Quantifying the impact of early calcite cementation on the reservoir quality of carbonate rocks: a 3d process-based model, *Adv. Water Resour.*, 2017, vol. 104, pp. 89–104.

Jahnert, R.J. and Collins, L.B., Characteristics, distribution and morphogenesis of subtidal microbial systems in Shark Bay, Australia, *Mar. Geol.*, 2012, vol. 303–306, pp. 115–136.

James, N.P., Narbonne, G.M., and Sherman, A.G., Molar tooth carbonates: Shallow subtidal facies of the Mid- to Late Proterozoic, *J. Sediment. Res.*, 1998, vol. 68, pp. 716–722.

Jelby, M.E., Grundvag, S.-A., Helland-Hansen, W., et al., Tempestite facies variability and storm-depositional processes across a wide ramp: Towards a polygenetic model for hummocky crossstratification, *Sedimentology*, 2020, vol. 67, pp. 742–781.

Kah, L.C. and Riding, R., Mesoproterozoic carbon dioxide levels inferred from calcified cyanobacteria, *Geology*, 2007, vol. 35, pp. 799–802.

Khabarov, E.M., Late Proterozoic reefs and Reef-type buildups in the southern part of eastern Siberia, *Geol. Geofiz.*, 1999, vol. 40, no. 8, pp. 1149–1169.

Kozlov, V.I., *Verkhnii rifei i vend Yuzhnogo Urala* (Upper Riphean and Vendian in the Southern Urals), Moscow: Nauka, 1982.

Kozlov, V.I., Puchkov, V.N., Krasnobaev, A.A., et al., The Arshinian, a new Riphean straton in the Southern Urals stratotype sections, in *Geologicheskii sbornik* (Geological Collection), Ufa: DizainPoligrafServis, 2011, pp. 52–56.

Krylov, I.N., *Rifeiskie i nizhnekembriiskie stromatolity Tyan'-Shanya i Karatau* (Riphean and Lower Cambrian Stromatolites in Tien-Shan and Karatau), Moscow: Nauka, 1967.

Krylov, I.N., *Stromatolity rifeya i fanerozoya SSSR* (Riphean and Phanerozoic Stromatolites in the Soviet Union), Moscow: Nauka, 1975.

Kuang, H-W., Review of molar tooth structure research, *J. Palaeogeogr*, 2014, vol. 3, pp. 359–383.

Kuang, H-W., Fan, Z.-X., Liu, Y.-Q., et al., Stromatolite characteristics of Mesoproterozoic Shennongjia Group in the northern margin of yangtze block, china, *China Geology*, 2019, vol. 3, p. 364.

Kuznetsov, V.G., Molar tooth structure–is a specific structure of the Riphean sediments, *Litosfera*, 2005, no. 4, pp. 136–150.

Kuznetsov, A.B., Semikhatov, M.A., Maslov, A.V., et al., New data on Sr- and C-isotopic chemostratigraphy of the Upper Riphean type section (Southern Urals), *Stratigr. Geol. Correl.*, 2006, vol. 14, no. 6, pp. 602–628.

Kuznetsov, A.B., Semikhatov, M.A., and Gorokhov, I.M., The Sr isotope chemostratigraphy as a tool for solving stratigraphic problems of the Upper Proterozoic (Riphean and Vendian), *Stratigr. Geol. Correl.*, 2014, vol. 22, no. 6, pp. 553–575.

Li, Z.X., Evans, D.A., and Halverson, G.P., Neoproterozoic glaciations in a revised global palaeogeography from the breakup of Rodinia to the assembly of Gondwanaland, *Sediment. Geol.*, 2013, vol. 294, pp. 219–232.

Lokier, S.W. and Junaibi, M.Al., The petrographic description of carbonate facies: are we all speaking the same language?, *Sedimentology*, 2016, vol. 63, no. 7, pp. 1843–1885.

Maslov, A.V., Bashkirian meganticlinorium: Late Riphean-Vendian hiatuses and possible transformations of basin provenances, *Litosfera*, 2020, no. 4, pp. 455–470.

Maslov, A.V., Krupenin, M.T., Gareev, E.Z., and Anfimov, L.V., *Rifei zapadnogo sklona Yuzhnogo Urala (klassicheskie razrezy, sedimento- i litogenez, minerageniya, geologicheskie pamyatniki prirody*) (Riphean on the western slope of the Southern Urals—Classical sections, sedimento- and lithogenesis, minerageny, and geological landmarks), Yekaterinburg: IGG UrO RAN, 2001, vol. 2.

Maslov, A.V., Olovyanishnikov, V.G., and Isherskaya, M.V., Riphean deposits on eastern, north-eastern, and northern periphery of the Russian Platform and western megazone of the Urals: lithostratigraphy, formation conditions and types of sedimentary succession, *Litosfera*, 2002, no. 2, pp. 54–95.

Maslov, A.V., Grazhdankin, D.V., Dub, S.A., et al., Sedimentology and geochemistry of the Uk Formation, Upper Riphean, the Southern Urals, *Litosfera*, 2019, vol. 19, no. 5, pp. 659–686.

Maslov, V.P., *Stromatolity* (Stromatolites), in *Tr. GIN Akad. Nauk SSSR*, 1960, no. 41, p. 188.

Molina, J.M., Alfaro, P., Moretti, M., and Soria, J.M., Soft-sediment deformation structures induced by cyclic stress of storm waves in tempestites (Miocene, Guadalquivir Basin, Spain), *Terra Nova*, 1998, vol. 10, pp. 145–150.

Monty, C., An autoecological approach of intertidal and deep-water stromatolites, *Ann. Société Géol. Belg.*, 1971, vol. 94, no. 3, pp. 265–276.

Myrow, P.M., Bypass-zone tempestite facies model and proximality trends for an ancient muddy shoreline and shelf, *J. Sediment. Petrol.*, 1992, vol. 62, pp. 99–115.

Myrow, P.M. and Southard, J.B., Tempestite deposition, *J. Sediment. Res.*, 1996, vol. 66, pp. 875–887.

Narbonne, G.M., James, N.P., Rainbird, R.H., and Morin, J., Early Neoproterozoic Tonian patch reef complexes Victoria Island Arctic Canada, in *Carbonate sedimentation and diagenesis in the evolving Precambrian World (SEPM Spec. Publ.*), Grotzinger, J.P. and James, N.P., Eds., 2000, vol. 67, pp. 164–177.

Parfenova, T.M. and Mel'nik, D.S., Geochemistry of the organic matter dispersion in the Uk Formation rocks (Upper Riphean, Southern Urals), in *Ot analiza veshchestva - k basseinovomu analizu* (From the Analysis of Matter to the Analysis of Basin), Yekaterinburg, 2020, pp. 190–192.

Petrov, P.Yu. and Semikhatov, M.A., Carbonate platforms: Shorikha Formation of the Turukhansk Uplift, Siberia, *Stratigr. Geol. Correl.*, 2009, vol. 17, no. 5, pp. 461–575.

Petrov, P.Yu., Molar tooth structures: Formation and specificity of carbonate diagenesis in the Late Precambrian, Middle Riphean Sukhaya Tunguska Formation of the Turukhansk Uplift, Siberia), *Stratigr. Geol. Correl.*, 2011, vol. 19, no. 3, pp. 247–267.

Planavsky, N. and Grey, K., Stromatolite branching in the Neoproterozoic of the Centralian Superbasin, Australia: an investigation into sedimentary and microbial control of stromatolite morphology, *Geobiology*, 2008, vol. 6, pp. 33–45.

Pollock, M.D., Kah, L.C., and Bartley, J.K., Morphology of molar-tooth structures in Precambrian carbonates: influence of substrate rheology and implications for genesis, *J. Sediment. Res.*, 2006, vol. 76, pp. 310–323.

Pratt, B.R., Molar-tooth structure in Proterozoic carbonate rocks: origin from synsedimentary earthquakes, and implications for the nature and evolution of basins and marine sediment, *Geology*, 1998, vol. 110, no. 8, pp. 1028–1045.

Puchkov, V.N., Sergeeva, N.D., and Krasnobaev, A.A., Stratigraphic scheme of the Riphean standard of the Southern Urals, *Geologiya. Izv. Otd. Nauk Zemle Prirodn. Resurs. AN RB*, 2017, no. 23, pp. 3–26.

Purkis, S.J., Rowlands, G.P., and Kerr, J.M., Unravelling the influence of water depth and wave energy on the facies diversity of shelf carbonates, *Sedimentology*, 2015, vol. 62, pp. 541–565.

Putevoditel geologicheskoi ekskursii po razrezam paleozoya i verkhnego dokembriya zapadnogo sklona Yuzhnogo Urala i Priural'ya (Geological Excursion Guidebook for Paleozoic and Upper Precambrian Sections on the Western Slope of the Southern Urals and Cis-Ural Region), Ufa, 1995.

Raaben, M.E., Riphean stromatolitic formations fringing the East European Platform, *Stratigr. Geol. Correl.*, 2007, vol. 11, no. 2, pp. 30–40.

Read, J.F., Carbonate platform facies models, *AAPG Bull.*, 1985, vol. 69, pp. 1–21.

Riding, R., Calcified cyanobacteria, in *Encyclopedia of Geobiology. Encyclopedia of Earth Sciences Series*, Reitner, J. and Thiel, V., Eds., Dordrecht: Springer, 2011a, p. 211–223.

Riding, R., The nature of stromatolites: 3,500 million years of history and a century of research, in *Advances in Stromatolite Geobiology*, Reitner, J. and Quéric, G. Arp., Eds., Heidelberg: Springer, 2011b, vol. 131, pp. 29–74.

Schopf, J.W., The fossil record of cyanobacteria, in *Ecology of Cyanobacteria II, Their Diversity in Space and Time*, Whitton, B.A., Ed., Berlin: Springer, 2012, pp. 15–36.

Seilacher, A. and Aigner, T., Storm deposition at the bed, facies, and basin scale: the geologic perspective, in *Cycles and Events in Stratigraphy*, Einsele, G., Ricken, W., and Seilacher, A., Eds., Berlin: Springer, 1991, pp. 249–267.

Semeniuk, V., Tidal flats, in *Encyclopedia of Coastal Science*, Finkl, C.W. and Makowski, C., Eds., Berlin: Springer, 2019, pp. 1708–1727.

Serebryakov, S.N., Peculiarities in the formation and distribuition of Riphean stromatolites in Siberia, in *Tr. GIN AN SSSR*, Moscow: Nauka, 1975, no. 200.

Sergeev, V.N., *Okremnennye mikrofossilii dokembriya: priroda, klassifikatsiya i biostratigraficheskoe znachenie* (Precambrian Silicified Microfossils: Nature, Classification, and Biostratigraphic Significance), Moscow: GEOS, 2006.

Sergeev, V.N., Semikhatov, M.A., Fedonkin, M.A., and Vorob'eva, N.G., Principal stages in evolution of Precambrian organic world: Communication 2. The Late Proterozoic, *Stratigr. Geol. Correl.*, 2010, vol. 18, no. 6, pp. 561–592.

Shields, G.A., "Molar-tooth microspar": A chemical explanation for its disappearance ~ 750 Ma, *Terra Nova*, 2002, vol. 14, pp. 108–113.

Shinn, E.A., Practical significance of birdseye structures in carbonate rocks, *J. Sediment. Petrol.*, 1968, vol. 38, pp. 215–223.

Smith, A.G., A review of molar-tooth structures with some speculations on their origin, in Belt Basin: Window to Mesoproterozoic Earth, MacLean, J.S. and J.W. Sears, Eds., *Geol. Soc. Am. Spec. Pap.*, 2016, vol. 522, pp. 71–99.

Smith, A., Cooper, A., Misra, S., et al., The extant shore platform stromatolite (SPS) facies association: a glimpse into the Archean?, *Biogeosciences*, 2018, vol. 5, pp. 2189–2203.

Stanevich, A.M., Puchkov, V.N., Kornilova, T.A., et al., Microfossils of the Southern Ural Riphean stratotype and Late Precambrian of Eastern Siberia (paleobiologic aspects), *Geol. Vest.*, 2018, no. 3, pp. 3–41.

Stratotip rifeya. Paleontologiya, paleomagnetizm (The Riphean Stratotype: Paleontology and Paleomagnetism), Moscow: Nauka, 1982.

Stratotip rifeya. Stratigrafiya. Geokhronologiya (The Riphean Stratotype: Stratigraphy and Geochronology), Moscow: Nauka, 1983.

Suosaari, E.P., Reid, R.P., Playford, P.E., et al., New multiscale perspectives on the stromatolites of Shark Bay, Western Australia, *Sci. Rep.*, 2016, vol. 6, p. 20557.

Swift, D.J.P., Figueiredo, A.G.Jr., Freeland, G.L., and Oertel, G.F., Hummocky cross-stratification and megaripples: a geological double standard?, *J. Sediment. Petrol.*, 1983, vol. 53, pp. 1295–1317.

Thorie, A., Mukhopadhyay, A., Mazumdar, P., and Banerjee, T., Characteristics of a Tonian reef rimmed shelf before the onset of Cryogenian: Insights from Neoproterozoic Kunihar Formation, Simla Group, Lesser Himalaya, *Mar. Petrol. Geol.*, 2020, vol. 117, p. 104393.

Tosti, F. and Riding, R., Fine-grained agglutinated elongate columnar stromatolites: Tieling Formation, ca 1420 Ma, North China, *Sedimentology*, 2017, vol. 64, pp. 871–902.

Turner, E.C., James, N.P., and Narbonne, G.M., Growth dynamics of Neoproterozoic calcimicrobial reefs, Mackenzie mountains, northwest Canada, *J. Sediment. Res.*, 1997, vol. 67, pp. 437–450.

Turner, E.C., James, N.P., and Narbonne, G.M., Taphonomic control on microstructure in Early Neoproterozoic reefal stromatolites and thrombolites, *Palaios*, 2000, vol. 15, pp. 87–111.

Vakarelov, B.K. and Ainsworth, R.B., and MacEachern J.A., Recognition of wave-dominated, tideinfluenced shoreline systems in the rock record: variations from a microtidal shoreline model, *Sediment. Geol.*, 2012, vol. 279, pp. 23–41.

Veis, A.F., Kozlov, V.I., Sergeeva, N.D., and Vorob'eva, N.G., Microfossils from the Upper Riphean type section (the Karatau Group of Southern Urals), *Stratigr. Geol. Correl.*, 2003, vol. 11, no. 6, pp. 550–572.

Wright, V.P., A revised classification of limestones, *Sediment. Geol.*, 1992, vol. 76, pp. 177–185.

Yang, B.C., Dalrymple, R.W., and Chun, S.S., Sedimentation on a wave-dominated, open-coast tidal flat, southwestern Korea: summer tidal flat - winter shoreface, *Sedimentology*, 2005, vol. 52, pp. 235–252.

Zaitseva, T.S., Gorokhov, I.M., Ivanovskaya, T.A., et al., Mössbauer characteristics, mineralogy and isotopic age (Rb–Sr, K–Ar) of Upper Riphean glauconites from the Uk Formation, the Southern Urals, *Stratigr. Geol. Correl.*, 2008, vol. 16, no. 3, pp. 227–247.

Zaitseva, T.S., Kuznetsov, A.B., Gorozhanin, V.M., et al., The lower boundary of the Vendian in the Southern Urals as evidenced by the Rb–Sr age of glauconites of the Bakeevo Formation, *Stratigr. Geol. Correl.*, 2019, vol. 27, no. 5, pp. 573–587.

Zaky, A.H., Brand, U., Buhl, D., et al., Strontium isotope geochemistry of modern and ancient archives: tracer of secular change in ocean chemistry, *Can. J. Earth Sci.*, 2019, vol. 56, no. 3, pp. 245–264.

Zhuravlev, A.Yu., Paleoecology of Cambrian reef ecosystems, in *The History and Sedimentology of Ancient Reef Systems*, Stanley, J.D., Ed., New York: Plenum Press, 2001, pp. 121–157.

Zhuravlev, A.Yu., Systematics and paleoecology of the Cambrian calcareous "algae", in *Vodorosli v evolyutsii biosfery* (Algae in the Biosphere Evolution), Moscow: PIN RAN, 2013, pp. 38–39.

Translated by D. Sakya